THE ROLE OF N-GLYCOSYLATION IN MEDIATING SARS-COV-2 SPIKE BINDING TO HUMAN ANGIOTENSIN-CONVERTING ENZYME 2 AND RECOGNITION BY ANTI-SPIKE MONOCLONAL ANTIBODIES

by

PAIGE LAMORE

(Under the Direction of Robert J. Woods)

ABSTRACT

The Coronavirus Disease 2019 (COVID-19) global pandemic caused by the Severe Acute Respiratory Syndrome Coronavirus 2 (SARS-CoV-2) virus emphasized the vital role of SARS-CoV-2 Spike (S) protein binding its angiotensin-converting enzyme 2 (ACE2) host cell receptor. Understanding the molecular features that influence the S-ACE2 interaction is essential for the development of effective anti-S therapeutics. While the receptor binding domain (RBD) of ACE2 is known to directly interact with ACE2, the precise influence of N-glycans on S and ACE2, in addition to specific RBD mutations is not fully understood. The S protein is a large viral surface protein that contains the Receptor Binding Domain (RBD) that directly binds to the ACE2 receptor, which allows conformational changes for host protease cleavage and viral infection. Thus, the strength of S-ACE2 binding affinity is a major factor of viral infection and transmission.

This thesis aims to elucidate how variations in glycosylation and predominant RBD mutations of the SARS-CoV-2 S glycoprotein influence interactions with receptor and antibody binding. Through a combination of structural analyses and *in vitro* binding assays via biolayer interferometry, this research provides insight into the molecular features that mediate the Spike-

ACE2 interaction in quantitative terms. Key results revealed that specific N-glycans on ACE2 and S mediated binding. Additionally, specific RBD mutations led to altered binding affinities observed in SARS-CoV-2 variants of concern (VOC) for ACE2 and monoclonal antibodies (mAbs). These findings advance our understanding of the factors that mediate therapeutic mAb binding to their target antigen, and the design parameters that should be considered as demonstrated in anti-S therapeutic mAb interactions.

INDEX WORDS: SARS-CoV-2, Spike protein, ACE2, N-Glycosylation, binding affinity, monoclonal antibody, CR3022, BLI

THE ROLE OF N-GLYCOSYLATION IN MEDIATING SARS-COV-2 SPIKE BINDING TO HUMAN ANGIOTENSIN-CONVERTING ENZYME 2 AND RECOGNITION BY ANTI-SPIKE MONOCLONAL ANTIBODIES

by

PAIGE LAMORE

BS, Agnes Scott College, 2018

A Thesis Submitted to the Graduate Faculty of The University of Georgia in Partial Fulfillment of the Requirements for the Degree

MASTER OF SCIENCE

ATHENS, GEORGIA

2025

THE ROLE OF N-GLYCOSYLATION IN MEDIATING SARS-COV-2 SPIKE BINDING TO HUMAN ANGIOTENSIN-CONVERTING ENZYME 2 AND RECOGNITION BY ANTI-SPIKE MONOCLONAL ANTIBODIES

by

PAIGE LAMORE

Major Professors:	Robert J. Woods
Committee:	Zachary A. Wood
	Kelley W. Moremen
	Stephen M. Tomkins

Electronic Version Approved:

Ron Walcott
Vice Provost for Graduate Education and Dean of the Graduate School
The University of Georgia
August 2025

DEDICATION

I dedicate this thesis to my great grandmother, Marie Antonia Fowler, who embodied the spirit of hard work, determination, and grace. Her unwavering perseverance in the face of life's obstacles has inspired my work and continues to drive my passion for contributing to scientific knowledge and improving quality of life.

ACKNOWLEDGEMENTS

I would like to thank my advisor, Dr. Robert Woods, for the valuable lessons and scientific insight I have received these last few years. Additionally, I thank my committee, Dr. Zachary Wood, Dr. Kelley Moremen, and Dr. Stephen Mark Tomkins for their advisement and guidance during my academic journey.

I would like to thank the Glycoscience Training Program (GTP) for funding from 2021-2022 and for providing me with the support and tools necessary to perform this work.

I would like to thank my friends and colleagues at the Complex Carbohydrate Research Center. Specifically, I appreciate members from the Woods, Wells, and Moremen lab for providing reagents and samples that were used to complete this work. Thank you to Digant Chopra for the samples used in my experiments. I also thank Yi Ji for providing the training and basis for this project. I am grateful to my fellow glycoscientists, Ashley Rogers, Naomi Hitefield-Garwood, David Steen, and Ashley Carter for supporting and creating positive memories during my time here.

I am grateful to my mother and father, Dee and Ron, for their unconditional love and support for my career as a scientist. Their work as first responders have been my inspiration and motivation to improve quality of life. I would like to thank my sister, Emilia, for always bringing a smile to my face and for reminding me to view science through a child's eyes with curiosity and open-mindedness. I would like to thank my brother, Colin, for always listening and providing laughter when it was most needed. Also, I am very appreciative to my aunt and uncle, Juanita and Charles Grayson, for always encouraging me to keep moving toward my goals and

uplifting me. Finally, thank you to my childhood best friend, McKenna Bertrand, for her loyal friendship and steadfast encouragement in my pursuit of advancing my scientific career.

AUTHOR CONTRIBUTIONS

Co-author Ye Ji from the Woods lab contributed the optimization of the bio-layer interferometry (BLI) assay conditions for ACE2-Spike.

Co-author Oliver C Grant from the Woods lab contributed the structural analyses for both S and ACE2 constructs.

Co-author Jeremy L Praissman from the Wells lab contributed the expression constructs and purification of ACE2 reagents.

Co-author Peng Zhao from the Wells lab contributed the mass spectrometry analyses and validation of S and ACE2 reagents used.

Co-author Digantkumar Chapala from the Moreman lab contributed the expression and purification of S.

Co-author Annapoorani Ramiah from the Moremen lab contributed the site-directed mutagenesis DNA plasmids for S and ACE2.

TABLE OF CONTENTS

Page

LIST OF FIGURES

Page

LIST OF TABLES

Page

CHAPTER 1

INTRODUCTION AND LITERATURE OVERVIEW

1.1 Overview of COVID-19 and SARS-CoV-2

Coronavirus Disease 2019 (COVID-19) is caused by viral infection with Severe Acute Respiratory Syndrome Coronavirus 2 (SARS-CoV-2), which rapidly spread and resulted in a global pandemic[1, 2]. SARS-CoV-2 mainly causes respiratory illness, ranging from mild to severe, but can be fatal in some individuals with comorbities[3]. While recent statistics from the World Health Organization (WHO) and Centers for Disease Control and Prevention (CDC) indicate a decrease from pandemic peaks, tracking of SARS-CoV-2-related cases, deaths, and vaccine effectiveness remain in effect as new variants emerge[1, 2].

The evolution of SARS-CoV-2 strains and lineages is driven by genetic point mutations within the viral genome[4-8]. SARS-CoV-2 strains can be listed as variants of concern (VOC) or variants of interest (VOI) for tracking by the WHO and CDC[1, 2] Such mutations influence viral protein structure, which mediates binding affinity for host receptors and antibody recognition, impacting overall changes in infectivity and transmissibility[4, 9-11].

1.2 SARS-CoV-2 Spike Glycoprotein: Structure and Function

A key step in the pathogenesis of SARS-CoV-2 is the binding of viral Spike (S) protein to its host cell receptor, angiotensin-converting enzyme 2 (ACE2), enabling protease cleavage, membrane fusion, and cellular entry (**Figure 1.1**). The S protein is a large trimeric surface glycoprotein that contains the Receptor Binding Domain (RBD), N-Terminal Domain (NTD),

and Fusion Peptide (FP). Previous and current dominant strains of SARS-CoV-2 show key mutations in the S proteins, displaying increased binding to ACE2, transmissibility, and or immune evasion (summarized **in Table 1.1**)[4, 9-11] The strength of S-ACE2 binding affinity is a major factor of viral infection and transmission, and inhibition of the S-ACE2 interaction is a major target for SARS-CoV-2 therapeutics[10-14] Thus, it is important to understand the factors that govern the S protein structure and function.

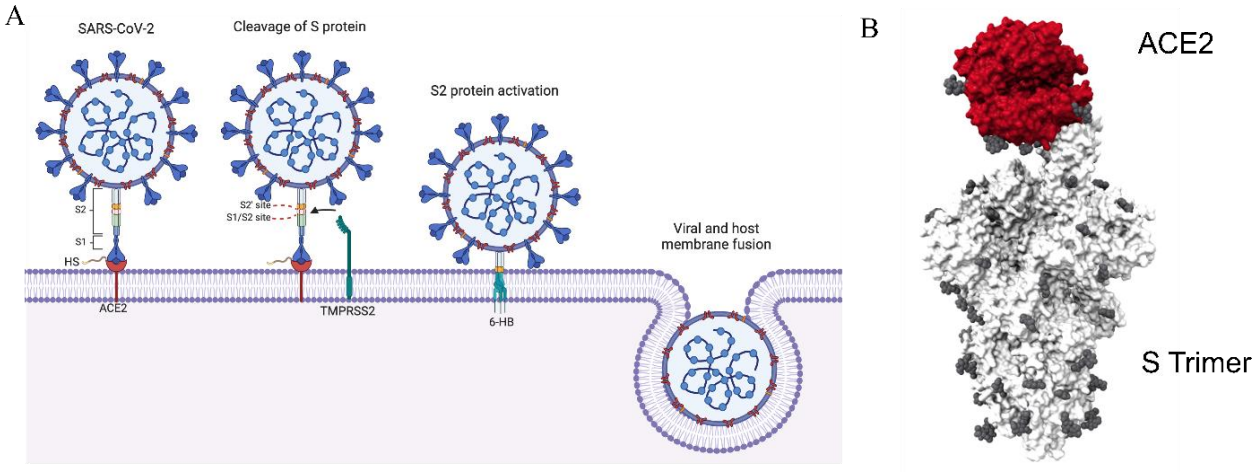

Figure 1.1 (A) Steps of SARS-CoV-2 pathogenesis (BioRender). (B) Glycosylated (gray) Spike trimer (white) of SARS-CoV-2 bound to human soluble ACE2 monomer (red) (PDB:7KJ2).

Table 1.1: Comparative Overview of Foundational SARS-CoV-2 Variants of Concern:

Infectivity and Transmissibility

Variant (WHO Label / Lineage)	Origin	Key Spike Mutations (Relevant)	Relative Transmissibility (vs. previous dominant)	Relative Infectivity (ACE2 Binding Affinity)	Key Characteristics & Notes
Wuhan (Original)	Dec 2019 (China)	D614G (emerged early 2020)	Baseline	High (Nanomolar range)	Initial strain, serves as baseline for comparison[15].
Alpha (B.1.1.7)	Sep 2020 (UK)	N501Y, 69-70del, P681H	~50-100% more transmissible than original[16-18]	Enhanced (N501Y increased ACE2 binding) [21]	Increased severity, rapid spread in late 2020/early 2021[21].
Beta (B.1.351)	May 2020 (South Africa)	K417N, E484K, N501Y	~50% more transmissible than original[19]	Enhanced (N501Y), but K417N/E484K complex effects[19]	Significant immune escape, some evidence of increased severity[20].
Gamma (P.1)	Nov 2020 (Brazil)	K417T, E484K, N501Y	~2.6 times more transmissible than wild-type[21, 22]	Enhanced (N501Y), complex effects from other mutations[21, 22]	Immune escape, associated with reinfections[21, 22].
Delta (B.1.617.2)	Oct 2020 (India)	L452R, T478K, P681R	Significantly more transmissible than Alpha/Beta[23]	Enhanced (L452R improves ACE2 binding) [23]	Highly transmissible, increased risk of hospitalization. Dominant globally in mid-2021[23].
Omicron (B.1.1.529)	Nov 2021 (South Africa)	Many (>30 in Spike), incl. N501Y, K417N, E484A, Q493R, T478K	~4.2 times more transmissible than Delta (early)[9, 20]	Generally enhanced (complex interplay of mutations) [9, 20]	High immune evasion, often associated with milder disease (due to prior immunity). Rapid global spread[9, 20].

Omicron Subvariants (e.g., BA.2, BA.4/BA.5, XBB, JN.1, XEC, KP.3.1.1)	Early 2022 - 2024 (Global)	Various, evolving from parent Omicron lineages	Continual growth advantage over preceding variants	Maintained/Slightly enhanced (e.g., BA.2.75/BA.2.75.2 stronger than BA.1)[9, 19]	Continued immune evasion, varying degrees of transmissibility advantage, often dominant in successive waves[9, 19, 23].

The RBD directly binds to the ACE2 receptor for the S trimer to undergo a conformational change from a "down" to an "up" state and allow host protease binding (**Figure 1.2)**, [24, 25]. SARS-CoV-2 variants of concern (VOC) RBD mutations influence S trimer conformation and N-glycan interactions with ACE2. Due to its trimeric structure, the S glycoprotein can exist in single-up, double-up, or triple-up conformations, depending on surrounding physiological conditions (**Figure 1.3)**[25]. While S can occupy up to three ligands simultaneously, the stoichiometry of bound ACE2 required for S2 protease cleavage to progression of viral fusion is not clear[26, 27].

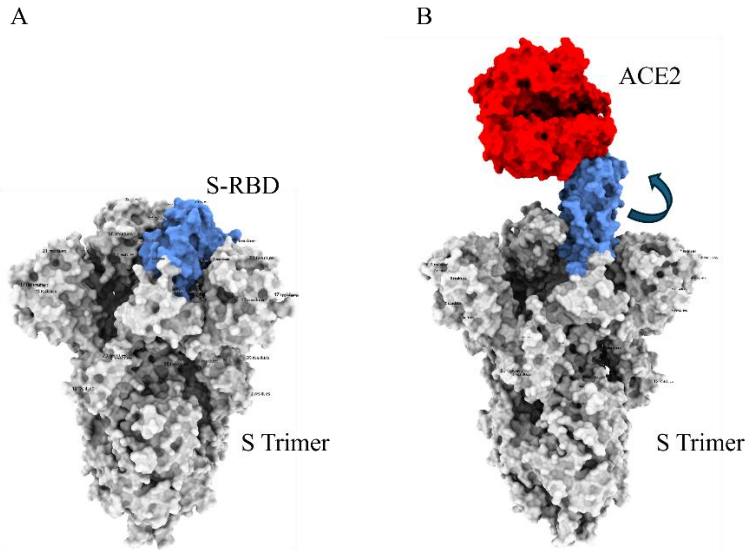

Figure 1.2 (A) Closed conformation of the SARS-CoV-2 S trimer (white) and RBD (blue) (PDB:6VXX). (B) Open conformation of Spike trimer (white) of SARS-CoV-2 and RBD (blue) bound to human soluble ACE2 monomer (red) (PDB:7Y9Z).

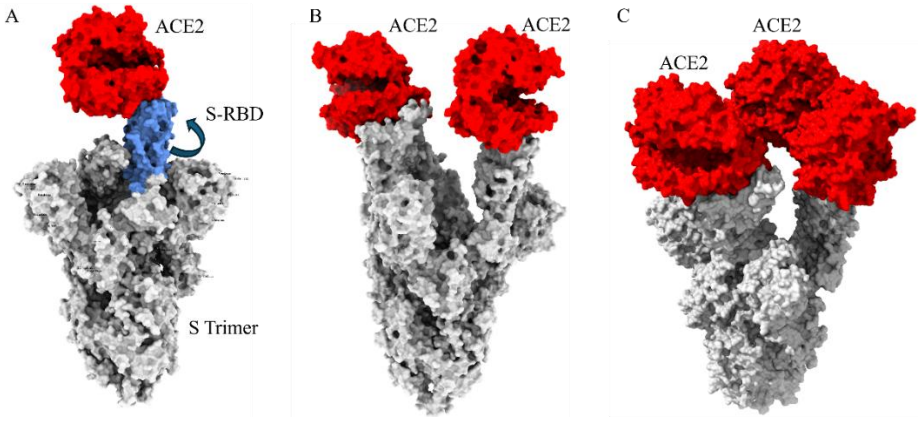

Figure 1.3 (A) Single-up, (B) double-up, and (C) triple-up conformations of Spike trimer (white) of SARS-CoV-2 and RBD (blue) bound to human soluble ACE2 monomer(s) (red) (PDB:7Y9Z. 7XCH, and 7XO8, respectively).

1.3 Angiotensin-Converting Enzyme 2 (ACE2) Host Receptor

The main role of ACE2 is to regulate blood pressure by counteracting ACE as part of the renin-angiotensin system (RAS), and is expressed at high level in the lungs, heart, kidneys, and brain[28]. ACE converts Angiotensin (Ang I) into Angiotensin II (Ang II), which acts as a vasoconstrictor[28]. The structure of ACE2 contains a receptor binding motif (RBM) and Peptidase Domain (PD) for Ang II into Angiotensin (1-7) (Ang1-7), which binds to MasR to promote vasodilation and decrease blood pressure[28]. When ACE2 activity becomes disrupted, such as individuals infected with SARS-CoV-2, Ang II builds up to result in increased blood pressure[28]. This expression pattern is reflected in the respiratory, cardio, and neurological symptoms observed during and post SARS-CoV-2 infection[3, 21]. The RBD of S in SARS-CoV-2 interacts directly with the RBM of ACE2, which illustrates the importance of studying the molecular features that modulate the S-ACE2 interaction.

1.4 The Role of *N*-Glycosylation During Viral Infection and Host-Pathogen Interactions

N-glycosylation is a post-translation modification (PTM) that involves the addition of a branched sugar, glycan, added to an asparagine residue within the consensus sequence "NxS" motif, where x is any amino acid (other than proline) and serine[29] N-glycosylation plays an important role in regulating cellular homeostasis[30, 31]. In mammalian cells, glycans serve a variety of functions, such as mediating antibodies from targeting "self" and "non-self" [30, 31]. However, pathogens can utilize glycans to evade detection by blocking antibodies from recognizing antigenic structures and or promoting protein stability to enhance binding affinity for their target receptor[11-13]. Demonstrating the specific importance of viral and host glycan interactions, the SARS-CoV-2 S trimer has 66 N-linked glycosylation sites, in which the

majority are conserved across SARS-CoV-2 strains[32]. Thus, N-glycosylation of the SARS-CoV-2 S trimer has an evolutionary basis to enhance binding to the ACE2 host cell receptor and evade antibody recognition (**Figure 1.1b)**[19].

Notably, ACE2 has seven N-glycans that regulate cell signaling and ACE2 stability[28]. Furthermore, N-glycosylation in mammalian proteins is inherently variable due to N-glycan processing as well as polymorphisms that result in loss or addition of specific glycosites[14]. In the context of SARS-CoV-2 infection, previous studies identified N-glycans located near the RBM of ACE2 and predicted contact the S trimer[33, 34]. While other studies have investigated how ACE2 N-glycans influence S-RBD binding affinity, their experimental design utilizes wildtype N-glycan processing cells[35]. However, how specific ACE2 N-glycosylation influence S binding affinity has not been investigated. Thus, it is crucial to consider how specific ACE2 N-glycans might interact with S.

1.5 *N*-Glycosylation and Sequence Variations Regulates Recognition and Efficacy of Anti-Spike Monoclonal Antibodies

The host adaptive immune system drives antigenic drift, or genetic modifications, in viral proteins for enhanced binding to the host cell receptor and reduced antibody recognition[4, 6]. This is reflected in the rapid rate of mutation in the receptor binding domain (RBD) of S in SARS-CoV-2 variants[4, 6, 8, 36]. SARS-CoV-2 variants of concern (VOC) RBD mutations influence S trimer conformation and N-glycan interactions with ACE2. Due to its trimeric structure, the S glycoprotein can exist in a single-up, double-up, or triple-up states, depending on surrounding physiological conditions[25]. While S can occupy up to three ligands simultaneously, the

stoichiometry of bound ACE2 required for S2 protease cleavage to progression of viral fusion is not clear and presents an additional challenge for design of anti-S mAbs[26, 27].

Concomitantly, emerging strains of SARS-CoV-2 gain many mutations within the S RBD that contribute to changes in ACE2 interactions and conformational dynamics[26]. For example, more recent biophysical analyses indicate that Omicron (BA.1) S trimer only presents in a single-up conformation to retain a prolonged monovalent binding to ACE2 while minimizing RBD exposure for reduced mAb recognition[27, 37]. Furthermore, SARS-CoV-2 strains display modified S glycan dynamics with ACE2[38, 39], suggesting mutations in BA.1 S RBD alter interactions with ACE2 glycans and evading S-shielding. However, it is not well understood how ACE2 N-glycan mutations affect mAb binding affinity for S, and consequently, their potency in select human individuals.

1.6 Overview of Dissertation

This dissertation describes research with the aim to provide insight into how Spike of SARS-CoV-2 and human ACE2 glycosylation modulate viral infection and evade antibody recognition in SARS-CoV-2 VOCs. In chapter 2, our studies will reveal differences in viral infectivity within the human population. In chapter 3, we investigate the impact of individual S RBD point mutations associated with SARS-CoV-2 variants and report the quantified values of binding affinity to ACE2. In chapter 4, we assay the binding of therapeutic mAbs with S and quantify the binding affinity for ACE2 and its N-glycan mutants. Together, these results will provide a better understanding of the S-ACE2 interaction and rationale for the design of mAb treatment for COVID-19.

CHAPTER 2

THE ROLE OF N-GLYCOSYLATION SARS-COV-2 SPIKE MEDIATING BINDING AFFINITY FOR HUMAN ANGIOTENSIN-COVERTING ENZYME 2

INTRODUCTION:

The severe acute respiratory syndrome coronavirus-2 (SARS-CoV-2) is a contagious virus that causes Coronavirus Disease (COVID-19) that led to a global pandemic. A critical step in SARS-CoV-2 infection is the interaction between the Spike (S) glycoprotein and its human angiotensin-converting enzyme 2 (ACE2) receptor, followed by cleavage of S by host transmembrane serine protease 2 (TMPRSS2) which enables viral membrane fusion and entry[3, 40]. Therefore, it is important to fully understand the molecular features that mediate the S-ACE2 interaction to provide a basis for the design of COVID-19 therapeutics.

Viruses are obligate parasites that depend on their host cell to complete their replication cycle and must circumvent immune recognition by developing their own mechanisms of defense[41, 42]. One method involves expression of glycans, or branched sugars, on viral proteins[29-31]. Glycans are a post-translational modification found on a wide range of proteins and play an important role in regulating cellular homeostasis[30, 31]. In mammalian cells, glycans serve a variety of functions, such as mediating antibodies from targeting "self" and "non-self" [30, 31]. Pathogens can utilize glycans to evade detection by blocking antibodies from recognizing

antigenic surfaces and or promoting protein stability to enhance binding affinity for their target receptor[11-13].

SARS-CoV-2 evolves from this type of selective pressure with the heavily glycosylated S trimer and suggests glycosylation plays a role in mediating receptor binding and immune masking of antigenic epitopes[19]. Prior analyses by mass spectrometry identified 66 N-glycans on S displaying microheterogeneity in composition[32, 34]. Notably, ACE2 has seven N-glycans that regulate cell signaling and ACE2 stability[28]. In context to SARS-CoV-2 infection, three ACE2 N-glycans located near the RBM of ACE2 are predicted to sterically hinder and shield S binding (**Figure 2.1)** [33, 34]. Notably, ACE2 N-glycosylation displays its own microhterogeneity[8, 14, 43, 44]. Thus, we aimed to investigate how N-glycosylation on S and ACE2 may influence their interactions.

Preliminary structural studies identified three glycosites, N90, N322, and N546 on ACE2 that are located near the receptor binding domain (RBD) of the S trimer[34] (**Fig. 2.2)**. Notably, T92I and N546D are human ACE2 polymorphisms that result in loss of glycosylation at N90 and N546 sites and may have implications for altered severity in SARS-CoV-2 infections[14]. Interestingly, molecular dynamic (MD) simulations revealed contacts N74 and N165 glycans on the S N-terminal domain with ACE2 N-glycans[34].

We hypothesize that specific glycosites on both trimeric S of SARS-CoV-2 and the ACE2 receptor form crucial contacts to mediate overall affinity. Our aim is to quantify in terms of binding affinity how specific N-glycans on both ACE2 and S influence the overall interaction by biolayer interferometry. Here, we find that N74 and N165 glycans on trimeric S contribute energetically

favorable interactions to promote ACE2 binding affinity. Alternatively, we reveal that ACE2 N-glycans N90, N322, and N546 form unfavorable interactions and reduce S binding affinity for ACE2. However, when performing a matrix, we observe additive relative binding energies with each mutation, apart from ACE2 N90S-S N74S/N165S interaction. We speculate that the human ACE2 polymorphisms that result in the N90 and N546 loss of glycosylation may impact severity of SARS-CoV-2 infection due to enhanced binding that is observed in our binding assays.

RESULTS

ACE2 N-Glycosylation is energetically unfavorable for S binding affinity for ACE2.

Initial structural analyses aimed to determine how ACE2 N-glycans interact with S to influence overall binding, and molecular dynamic (MD) simulations predicted ACE2 N90, N322, and N546 glycans directly interact with the S RBD and S N-glycans[34] (**Figure 2.1 A)**. Therefore, site-directed mutagenesis for specific N-glycan removal and biolayer interferometry were employed to observe how ACE2 N-glycans located nearby the S RBD may mediate overall binding affinity. Both ACE2 and S trimer, provided by collaborators, were expressed in HEK293S (GnTI-) cells. The absence of N-acetyl-glucosaminyltransferase I results in addition of only the restricted oligomannose form of glycans achieving a uniform glycan expression and molecular weight for quantifying binding affinities. The removal of ACE2 N90, N322, and N546 site-directed point mutagenesis resulted in increased binding affinity of S for ACE2, indicating that ACE2 N-glycosylation interacts unfavorably with S (**Figure 2.1 B&C).**

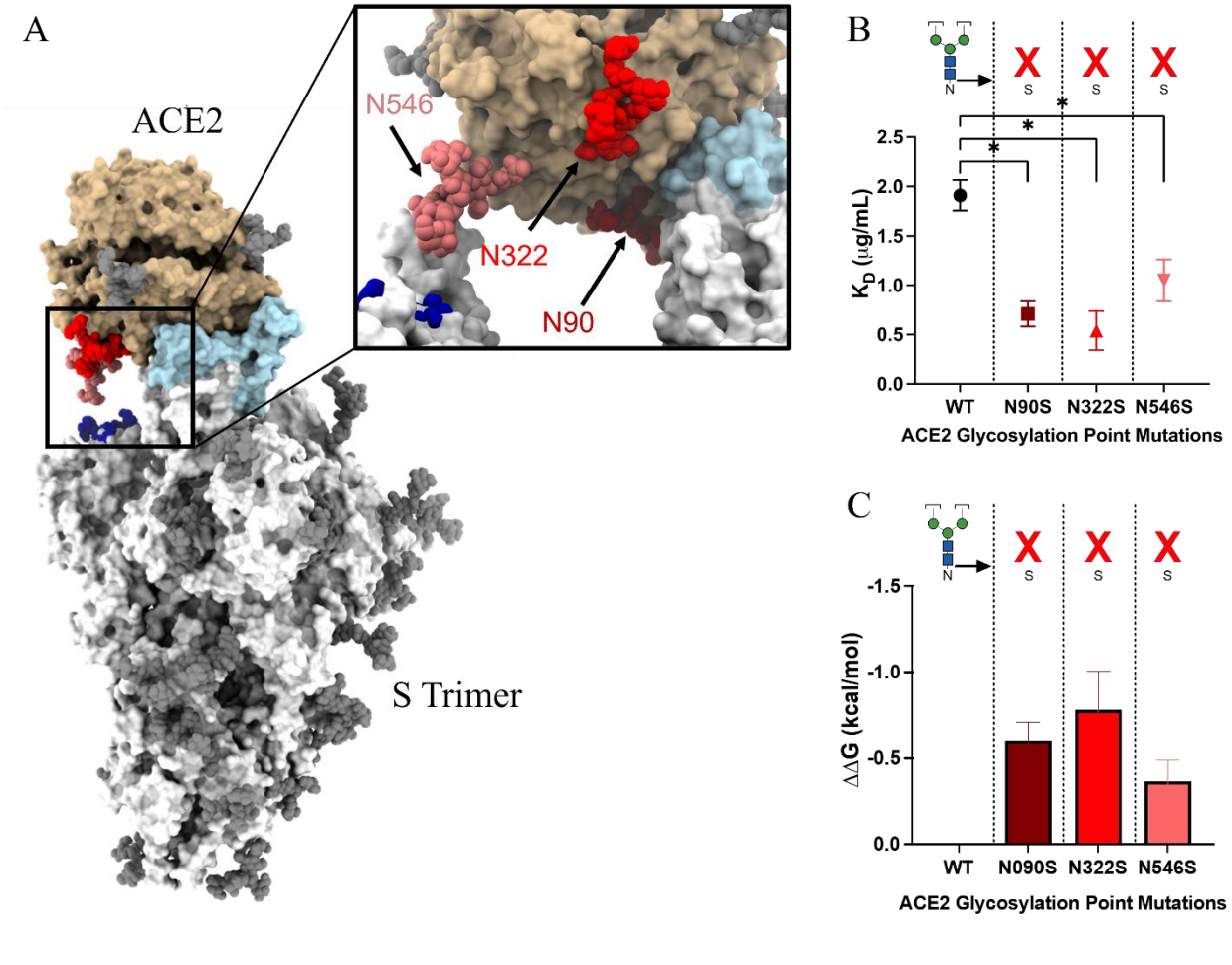

Figure 2.1 (A) Spike trimer (white) of SARS-CoV-2 bound to human soluble ACE2 monomer (wheat), ManAc5 N90 (dark red), N322 (red), N546 (pink) (PDB:7KJ2). (B) Dissociation constants (K_d) of S (D614G) binding ACE2 N-glycan mutants. (C) Relative binding energy of ACE2 N-glycan mutants binding S using $\Delta\Delta G = RT\ln(K_d/K_{d\ \text{Spike (D614G)}})$ * $p<0.05$, ** $p<0.005$, *** $p<0.0005$ for Dunnett's multiple comparisons test relative.

Table 2.1: Effect of ACE2 point mutations on K_d binding Spike WT by BLI.

ACE2 mutations[a]	K_d[b]	Fold Enhancement	Relative Binding Free Energy[c]
WT	1.99 ± 0.18	1.0	0.00 ± 0.06
N90S	0.76 ± 0.12[d]	2.6	-0.58 ± 0.10
N322S	0.54 ± 0.35[d]	2.0	-0.78 ± 0.21
N546S	1.05 ± 0.36[d]	1.6	-0.38 ± 0.17

[a]Expressed in HEK293 cells. [b]Average values (μg/mL) ± one standard deviation (n=3). [c]ln kcal/mol, from $\Delta\Delta G = RT\ln(K_d/K_{d\ \text{Spike (D614G)}})$. [d]$p < 0.05$.

N-Glycosylation on Trimeric Spike are Favorable for Binding Affinity to ACE2.

In addition to ACE2 N-glycosylation, our previous structural analyses sought to understand how S N-glycans might impact its binding affinity for ACE2. Previously, molecular dynamic (MD) simulations predicted S N74 and N165 glycans to interact with ACE2 and ACE2 N-glycans (**Figure 2.2A**). Based on this analysis, we performed binding assays in a similar manner using S protein N-glycan mutants to determine how S N74 and N165 glycans influence S-ACE2 binding affinity. Compared to S wildtype, the S N74K and N165Q mutants did not alter binding affinity for ACE2 (**Figure 2.2B&C**). However, the N165Q/N74K double mutant significantly decreased S binding affinity for ACE2 (**Figure 2.2B&C**). Thus, our binding studies suggest a role for S N165 and N74 glycans enhancing binding affinity for ACE2.

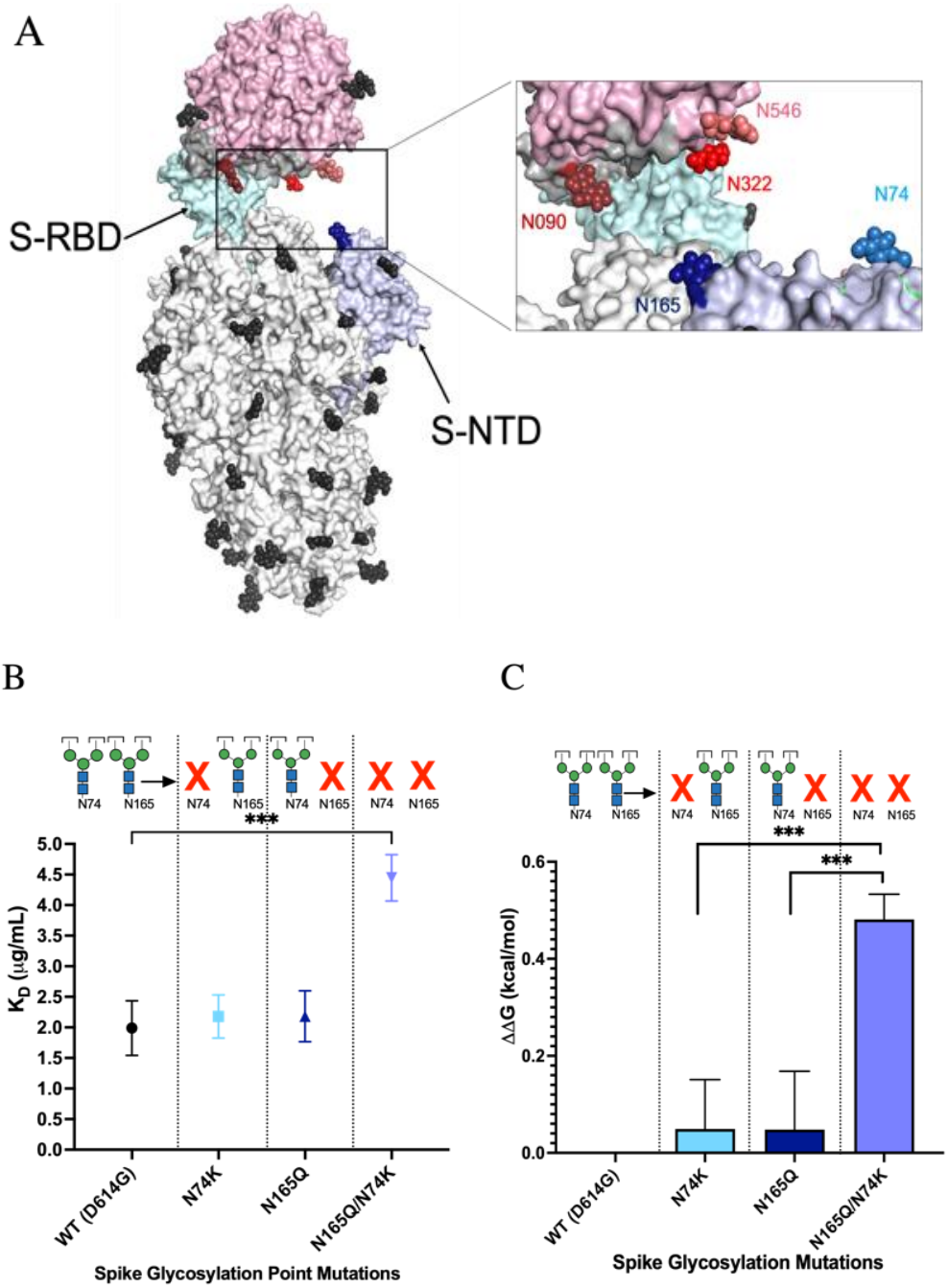

Figure 2.2 (A) N74 (light blue) and N165 (dark blue) on Spike trimer (white) of SARS-CoV-2, RBD (cyan) and NTD (cornflower), bound to human soluble ACE2 monomer (Pink), N90 (dark red), N322 (red), N546 (pink) (PDB:7KJ2). (B) Dissociation constants (K_d) of ACE2 WT

binding S (D614G) or N-glycan mutants. (C) Relative binding energy of ACE2 WT binding S (D614G) and N-glycan mutants using $\Delta\Delta G = RT\ln (K_d/K_{d\ \text{Spike (D614G)}})$ * $p<0.05$, ** $p<0.005$, *** $p<0.0005$ for Dunnett's multiple comparisons test relative.

Table 2.2: Effect of Spike point mutations on K_d binding ACE2 WT by BLI.

Spike mutations[a]	K_d[b]	Fold Enhancement	Relative Binding Free Energy[c]
WT	1.99 ± 0.18	1.0	0.00 ± 0.06
N74K	2.15 ± 0.38	0.92	0.04 ± 0.11
N165Q	2.19 ± 0.29	0.91	0.05 ± 0.08
N165Q/N74K	4.45 ± 0.38[d]	0.45	0.48 ± 0.05

[a]Expressed in HEK293 cells. [b]Average values (μg/mL) ± one standard deviation (n=3). [c]ln kcal/mol, from $\Delta\Delta G = (K_d/K_{d\ \text{Spike (D614G)}})$. [d]$p < 0.0005$.

ACE2 and S Trimer Glycosylation Mediate Protein Surface and Glycan-Glycan Interactions

Following the binding analyses of individual glycosites on ACE2 and S trimer, we continued our binding assays in a matrix using both ACE2 and S N-glycans mutants to quantify the relative binding energy contributed to the ACE2-S interaction. Our studies reveal that ACE2 N322S and N546S binding to S N74K and N165Q normalize the binding energy to S wildtype

binding ACE2 wildtype (**Figure 2.2A&B**). Interestingly, ACE2 N90S binding S N74K and N165Q individually follows a similar pattern apart from S N165Q/N74K with a significant increase in relatively binding energy or more energetically unfavorable interaction (**Figure 2.2A&B**). This was an unexpected result based on previous studies[4, 6, 9, 10, 45] and further analyses will need to be performed to fully understand how the ACE2 N90 glycan may energetically offset the S N165Q/N74K mutation.

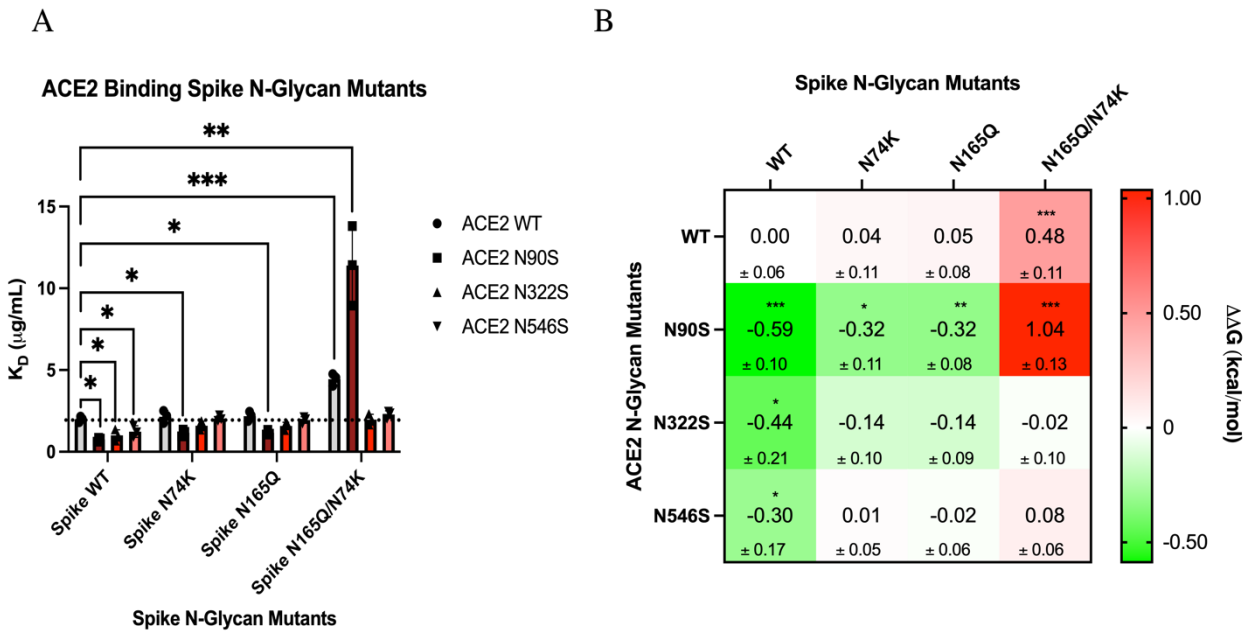

Figure 2.3 (A) Dissociation constants (K_d) and (B) relative binding energy of Spike glycosylation mutants binding ACE2 N-glycan mutants using $\Delta\Delta G = RT\ln(K_d/K_{d\ \text{Spike (D614G)}})$ * $p<0.05$, ** $p<0.005$, *** $p<0.0005$ for Dunnett's multiple comparisons test relative to ACE2 WT, Spike WT, and ACE2 mutants, respectively.

Table 2.3: Effect of Spike point mutations on K_d binding ACE2 point mutations by BLI.

ACE2 mutations[a]	Spike mutations[a]	K_d[b]	Gibbs Free Energy[c]	Relative Binding Free Energy[d]
WT	WT	1.99 ± 0.18	7.88 ± 0.06	0.00 ± 0.06
	N74K	2.15 ± 0.38	7.84 ± 0.11	0.04 ± 0.11
	N165Q	2.19 ± 0.29	7.82 ± 0.08	0.05 ± 0.08
	N165Q/N74K	4.45 ± 0.38[f]	7.40 ± 0.05	0.48 ± 0.05
N90S	WT	0.76 ± 0.12[e]	8.46 ± 0.10	-0.59 ± 0.10
	N74K	1.17 ± 0.20[e]	8.20 ± 0.11	-0.32 ± 0.11
	N165Q	1.17 ± 0.15[e]	8.20 ± 0.11	-0.32 ± 0.08
	N165Q/N74K	11.39 ± 2.43[g]	6.84 ± 0.13	1.04 ± 0.13
N322S	WT	1.00 ± 0.35[e]	8.31 ± 0.21	-0.44 ± 0.21
	N74K	1.60 ± 0.27[e]	8.01 ± 0.10	-0.14 ± 0.10
	N165Q	1.59 ± 0.23	8.02 ± 0.09	-0.14 ± 0.09
	N165Q/N74K	1.96 ± 0.33	7.89 ± 0.10	-0.02 ± 0.10
N546S	WT	1.24 ± 0.36[e]	8.18 ± 0.17	-0.30 ± 0.17
	N74K	2.04 ± 0.17	7.86 ± 0.05	0.01 ± 0.05
	N165Q	1.94 ± 0.20	7.89 ± 0.06	-0.02 ± 0.06
	N165Q/N74K	2.28 ± 0.23	7.80 ± 0.06	0.08 ± 0.06

[a]Expressed in HEK293 cells. [b]Average values (μg/mL) ± one standard deviation (n=3). [c]ln kcal/mol, from $\Delta G = -RT\ln(K_d)$. [d]ln kcal/mol, from $\Delta\Delta G = RT\ln(K_{d1}/K_{SpikeWT})$. [e]$p < 0.05$. [f]$p < 0.005$. [g]$p < 0.0005$.

DISCUSSION

Our findings demonstrate the role of site-specific N-linked glycans on SARS-CoV-2 S trimer and soluble human ACE2 host cell receptor interactions. We used BLI to quantify binding affinities of site-specific glycosylation mutants, we determined the impact of N-glycosites on the trimeric S-ACE2 interaction. Our results indicate essential roles for glycosylation mediating ACE2 receptor binding. The fact that T92I and N546D are human ACE2 polymorphisms suggests these glycan interactions may influence disease phenotypes observed across the human population[14].

The heavily glycosylated S trimer of SARS-CoV-2 and related MERS coronaviruses are distinct from other classes of viruses which highlights the important of understanding how N-glycosylation on S influences binding with its glycosylated ACE2 receptor[46]. Prior structure-guided analyses of S and ACE2 interactions predicted interaction between ACE2 N90 and N322 glycans with the S RBD, and ACE2 N546 with N74 glycan. Alternatively, the S N165 was predicted to interact directly with the ACE2 receptor binding motif (RBM). Here, we utilize structure-guided site-directed mutagenesis of specific N-glycans on these glycoproteins and the impact of their binding affinities in terms of K_d and relative binding energy ($\Delta\Delta G$) to reveal the individual energetic contributions of ACE2 and S N-glycans and overall implications of mutations that result in loss of glycosylation observed in nature.

We determined that ACE2 N90, N322, and N546 glycans are unfavorable for S trimer binding affinity. This observation aligns with previous MD simulation analyses and previous studies that suggest ACE2 N-glycosylation "shields" and sterically hinders S binding[34, 47]. Importantly, ACE2 polymorphisms T92I and N546D result in the loss of glycosylation at N90

and N546[14]. Thus, the observed increase in S binding affinity for N90S and N546S imply that individuals with these mutations may be more susceptible to infection.

Alternatively, trimeric S N-glycosylation enhanced binding affinity for ACE2. Specifically, S N165 and N74 glycans appear to be crucial contacts with ACE2 and its N-glycans to stabilize the open conformation. While previous studies imply a role for N165 to promote S stability in the open conformation and improving binding affinity[33], there has not been a reported Kd for either the N165 or N74 glycan mutant. Here, our binding assays of S N165Q and N74K showed significantly reduced binding affinity for ACE2 only when both were absent, supporting the initial proposal that N165 and N74 on S are necessary to expose the S RBD in its open formation for enhanced binding affinity for ACE2.

To understand the energetic contribution of individual N-glycans on ACE2 and S, we performed our binding assays in a matrix with the N-glycan variants normalized to ACE2 wildtype-S wildtype binding affinity, reported in terms of relative binding energy (ΔΔG). ACE2 N322S and N546S followed a pattern with S N74K, N165Q, and N165Q/N74K mutants to reach binding affinities approximate to wildtype. However, ACE2 N90S binding S N165/N74K with an increased unfavorable energy was an unexpected result. Previous studies predicted that ACE2 N546 made contacts with S N165 and N74[19]; therefore, we would predict that there would be a less favorable interaction with the respective mutants. Thus, further studies need to be performed to understand the ACE2 N90 interaction with S. However, all together, these findings provide insights into how N-glycans influence SARS-CoV-2 receptor binding.

The data reported here, combined with similar studies, provides context for the understanding of antibody-S interactions and how N-glycosylation potentially influences the

design of SARS-CoV-2 therapeutics. However, considerable work remains to fully understand the role of glycans in SARS-CoV-2 infection and pathogenicity. While HEK293-expressed S and ACE2 restricted to the oligomannose form provide a useful and controlled basis for study, site occupancy can change due to varied N-glycosylation processing by cell type[35]. Thus, binding assay analysis of Spike trimer from SARS-CoV-2 pseudovirus and patient-derived SARS-CoV-2 virions need to be performed to determine the overall impact of N-glycosylation on the S-ACE2 interaction. Ultimately, detailed structure and sequence analyses of emerging variants in S and ACE2 glycosylation variants and how they might influence binding are important for therapeutic design.

METHODS

Generation of Expression Constructs Encoding Wild Type and Mutant Forms of Spike and ACE2:

Expression constructs for mutant forms of Spike (D614G, D614G/N74K, D614G/N165Q, and D614G/N165Q/N74K) or ACE2 (N090S, N322S, and N546S) were generated using New England BioLabs Q5 Mutagenesis Kit (cat#0554S). The primers for each mutation were designed using NEBaseChanger program (https://nebasechanger.neb.com) and plasmid DNA preparations were generated for expression in HEK293S (GnTI-) cells (ATCC).

Expression and Purification Spike and ACE2:

Wild type and mutant forms of Spike and ACE2 proteins were, kindly provided by the Moremen and Wells lab, expressed as soluble secreted proteins by transient transfection of suspension cultures in HEK293S (GnTI-) cells maintained at 0.5–3.0x10^6 cells/ml in a humidified CO_2 platform shaker incubator at 37°C with 50% humidity and 125 rpm. Transient transfection was performed at a cell density of 2.5-3.0x10^6 cells/ml in expression medium comprised of a 9:1 ratio of Freestyle^{TM}293 expression medium (Thermo Fisher Scientific, Waltham MA) and EX-Cell expression medium including Glutmax (Sigma-Aldrich). Transfection was initiated by the addition of plasmid DNA and polyethyleneimine as transfection reagent (linear 25-kDa polyethyleneimine, Polysciences, Inc., Warrington, PA). Cell cultures were diluted with an equal volume of fresh media supplemented with valproic acid (2.2 mM final concentration) twenty-four hours post-transfection and protein production was continued for an additional 5 days at 37°C, 5% CO_2 with 125 rpm shaking. Cell cultures were harvested, clarified by sequential centrifugation at 1200 rpm for 10 min and 3500 rpm for 15 min at 4°C, and passed through a 0.8 μM filter (Millipore, Billerica, MA). The protein preparations were adjusted to contain 20 mM HEPES, 20 mM imidazole, 300 mM NaCl, pH 7.5, and subjected to Ni-NTA Superflow (Qiagen, Valencia, CA) chromatography using a column pre- equilibrated with Buffer I (20 mM HEPES, 300 mM NaCl, 20 mM imidazole, pH 7.5). The sample was loaded onto the column, washed with 3 column volumes of Buffer I, washed with 3 column volumes of Buffer II (20 mM HEPES, 300 mM NaCl, 50 mM imidazole) and eluted with Elution Buffer (20 mM HEPES, 300 mM NaCl, 300 mM imidazole, pH 7.0). The elution sample was concentrated using a 10 kDa

molecular mass cut-off ultrafiltration pressure cell (Millipore, Billerica, MA). Purified Spike and ACE2 proteins from HEK293S (GnTI-) was added to a Superdex G-200 gel filtration column (GE Healthcare) pre-equilibrated and eluted with Gel Filtration Buffer (20 mM HEPES, 100 mM NaCl, 0.05% sodium azide, pH 7.0) The eluted protein was stored at 4°C or 20°C. Prior to use the protein was thawed on ice and centrifuged at 8000 rcf for 20 minutes and supernatant was collected.

Biolayer Interferometry Binding Assays:

Spike (WT or mutants) were immobilized onto amine reactive "second-generation" biosensors (AR2G, Cat#: 18-5092, Pall ForteBio Corp., Menlo Park, CA, USA) by activation with 20mM EDC and 10mM sulfo-NHS solution for 1800s. Spike (20 μg/mL) was coupled to biosensors for 1800s, followed by quenching in 1M ethanolamine (pH8.5) for 600s. The immobilization resulted in a loading signal of approximately 1.5 nm.

Binding experiments were performed in PBST buffer (1xPBS with 0.1% Tween-20 at pH7.4, at 25°C), EDC (1-ethyl-3-(3-dimethylaminopropyl)carbodiimide hydrochloride Prod# 22980, Thermo Scientific, Rockford, IL, USA), Sulfo-NHS (Sulfo-NHS (N-hydroxysulfosuccinimide), Prod#24510, Thermo Scientific, Rockford, IL, USA), 10xPBS (10x Phosphate Buffered Saline, Cat#:1610780, Bio-Rad, Hercules, CA, USA), Ethanolamine (Cat# 110167, Sigma- Aldrich, St. Louis, MO, USA), Amine Reactive Second Generation biosensors (AR2G, Cat#: 18-5092, Pall ForteBio Corp., Menlo Park, CA, USA).

Direct binding constants (K_d) were measured using a BioLayer Interferometer (BLI) Octet Red 384 system (Pall ForteBio Corp., Menlo Park, CA, USA) and data was acquired using ForteBio Data Acquisition 8.2 software (Pall ForteBio Corp., Menlo Park, CA, USA). A baseline reading was collected for 120s in PBST Buffer only; then, both association and dissociation responses were detected for 600s. WT ACE2 was prepared in two- fold serial dilution in PBST from 0 to 80 µg/mL, and binding recorded in replicates of three. ACE2 mutants were similarly prepared in two-fold serial dilution in PBST but employed a concentration range of 0 to 20 µg/mL to obtain a more linear fit. Binding constants were calculated using Prism 10 (GraphPad Prism, USA) assuming a site- specific 1:1 binding model.

Structural Analyses:

Spike-ACE2 complex (PDB:7KJ2) modeled in ManAc5 N-glycans using Glycam Glycoprotein Builder (https://glycam.org/).

CHAPTER 3

THE EFFECT OF SARS-COV-2 SPIKE SEQUENCE VARIATIONS ON AFFINITY FOR HUMAN ANGIOTENSIN-CONVERTING ENZYME 2

INTRODUCTION

Severe acute respiratory syndrome coronavirus-2 (SARS-CoV-2) causes Coronavirus Disease (COVID-19). The COVID-19 global pandemic was a result of the high transmission rate of SARS-CoV-2 between human host and resulted in many deaths or long-term consequences to the population. SARS-CoV-2 infection involves the initial interaction between the Spike (S) viral glycoprotein and the human angiotensin-converting enzyme 2 (ACE2) receptor, which leads to viral fusion to the host cell membrane and infection. Thus, the S glycoprotein is a promising target for developing therapies and vaccines to combat SARS-CoV-2, and it is important to understand the molecular features that govern the interaction between S and the ACE2 host cell receptor.

As obligate parasites, viruses rely on the host cell to replicate and spread infection[7]. Therefore, viruses must evolve to enhance binding to their host cell surface and evade immune recognition to promote their replicative cycle[41, 42]. A significant component of SARS-CoV-2 evolution involves amino acid mutations within their receptor binding domain (RBD) to enhance binding affinity for their host cell surface receptor and reduce antibody binding[4, 6, 8, 36]. The S RBD of SARS-CoV-2 has gained many mutations throughout previous circulating variants[4, 6, 9, 10, 45

(**Figure 3.1 A&B**), which has resulted in changes in binding affinity for the human ACE2 receptor[4, 6, 9, 10, 45]. Alternatively, previous studies show increased immune escape from SARS-CoV-2 variants from S RBD mutations[4, 6, 9, 10, 45]. However, it is not fully understood the extent to which these S RBD mutations energetically contribute to the ACE2 interaction.

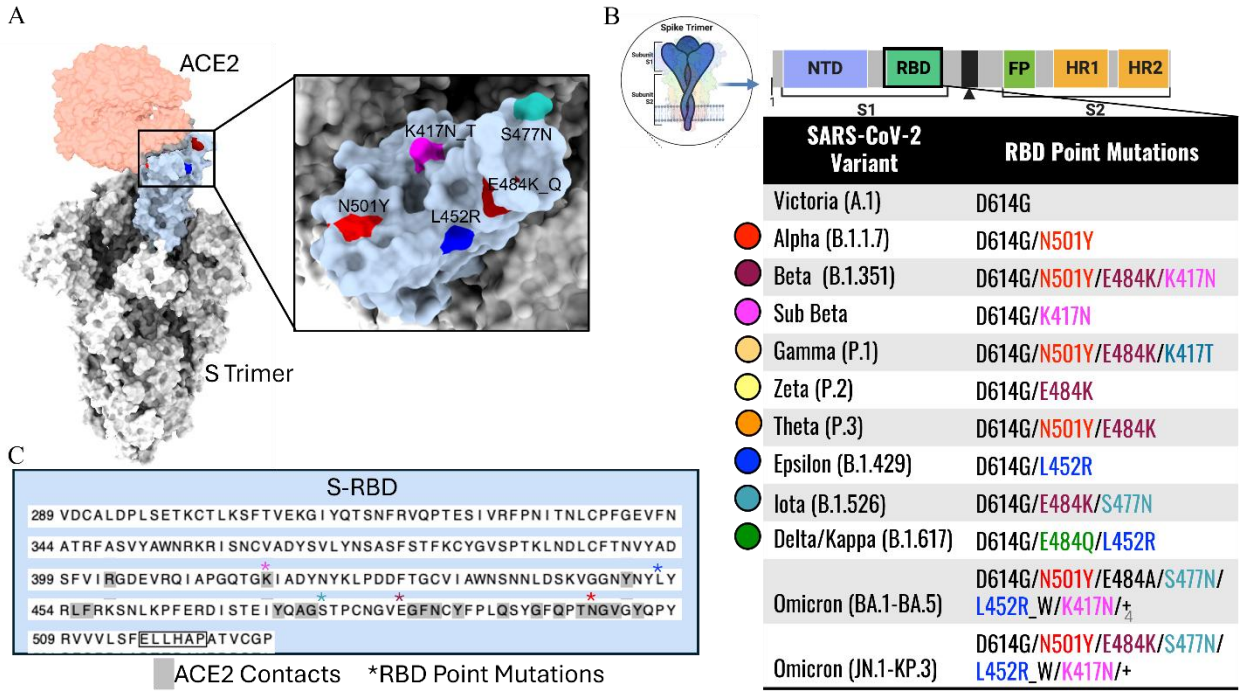

SARS-CoV-2 Variant	RBD Point Mutations
Victoria (A.1)	D614G
Alpha (B.1.1.7)	D614G/N501Y
Beta (B.1.351)	D614G/N501Y/E484K/K417N
Sub Beta	D614G/K417N
Gamma (P.1)	D614G/N501Y/E484K/K417T
Zeta (P.2)	D614G/E484K
Theta (P.3)	D614G/N501Y/E484K
Epsilon (B.1.429)	D614G/L452R
Iota (B.1.526)	D614G/E484K/S477N
Delta/Kappa (B.1.617)	D614G/E484Q/L452R
Omicron (BA.1-BA.5)	D614G/N501Y/E484A/S477N/L452R_W/K417N/+
Omicron (JN.1-KP.3)	D614G/N501Y/E484K/S477N/L452R_W/K417N/+

Figure 3.1 (A) Spike trimer (white) of SARS-CoV-2, RBD (light blue) bound to human soluble ACE2 monomer (salmon) (PDB:7KJ2). (B) RBD point mutations of SARS-CoV-2 variants B.1.17-KP.3 (BioRender).

Here, we demonstrate that specific RBD mutations in S of SARS-CoV-2 variants energetically contribute to enhanced binding affinity to ACE2. The goal of this study is to quantify the binding affinity of S RBD mutants of SARS-CoV-2 variants to ACE2 using site directed mutagenesis and biolayer interferometry. Our investigation reveals that specific S RBD mutations only enhance binding affinity for ACE2. Interestingly, the individual K417N mutation observed in the SARS-CoV-2 Beta (B.1.315) variant displayed a significant decrease in binding affinity, suggesting that other mutations (N501Y, and E484K) energetically offset this unfavorable mutation. These findings reveal the consequences of selective pressure on the S glycoprotein and provide a framework for therapeutic design for evolving SARS-CoV-2 variants.

RESULTS

S RBD mutations N501Y and E484K/Q associated with SARS-CoV-2 variants enhance binding affinity for ACE2.

Previous circulating variants of SARS-CoV-2 gained mutations in the S RBD[4, 6, 9, 10, 45]. Understanding how mutations play a role in the virus evolving away from mAb recognition is important for the development of novel SARS-CoV-2 therapeutics (**Figure 2.1 A)**. Therefore, we utilized site-directed mutagenesis to reproduce mutations found in SARS-CoV-2 variants and biolayer interferometry (BLI) to determine how individual RBD point mutations influence S binding affinity for ACE2. The ACE2 and S trimer were expressed in HEK293S (GnTI-) for a restricted, uniform oligomannose expression and molecular weight for quantifying binding affinities. Here, we report that mutations in SARS-CoV-2 variants Alpha, Zeta, Theta, Iota, and Delta/Kappa significantly enhance binding affinity for ACE2 (**Figure 3.2 B&C)**. This result

suggests that variants containing N501Y (positive to neutral charge) and E484K/Q (negative to positive or neutral charge) mutations contribute more favorable interaction with ACE2 and agrees with structural analyses of ACE2 contact sites on the S RBD.

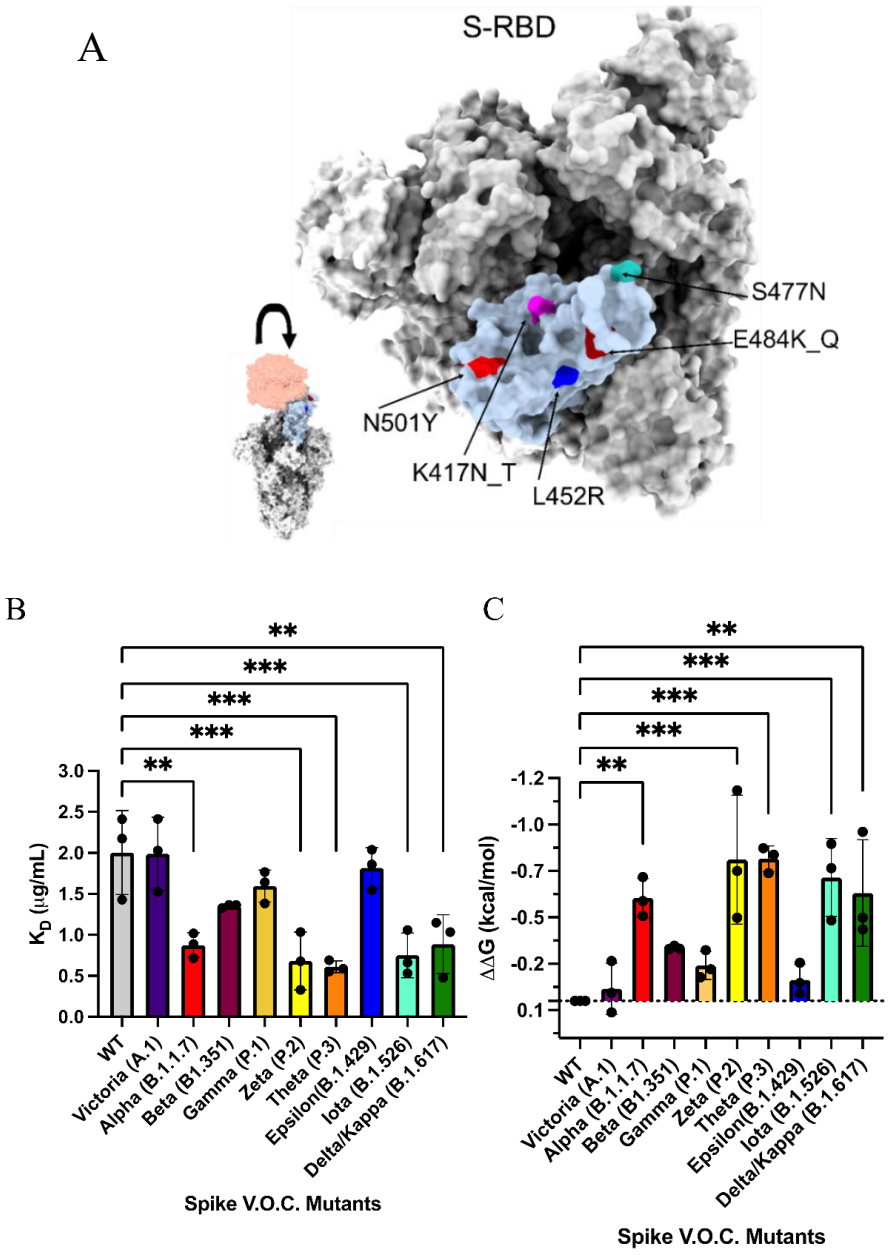

Figure 3.2 (A) Rotated view of Spike trimer (white) of SARS-CoV-2, RBD (light blue) point mutations N501Y (red), K417N_T (magenta), L452R (blue), E484K_Q (dark red), S477N (cyan) (PDB:7KJ2). (B) Dissociation constants (K_d) and (C) relative binding energy of S RBD point mutations of SARS-CoV-2 variants binding affinity ACE2 WT using $\Delta\Delta G = RT\ln(K_d/K_{d\ Spike\ WT})$ * $p<0.05$, ** $p<0.005$, *** $p<0.0005$ for Dunnett's multiple comparisons test.

The K417N point mutation observed in SARS-CoV-2 Beta (B.1.315) is unfavorable for S binding affinity for ACE2 SARS-CoV-2.

The SARS-CoV-2 Beta (B.1.315) variant contains the N501Y, E484K, and K417N mutations[4, 6, 9, 10, 45]. We hypothesized K417N would show enhanced binding affinity for ACE2. However, the Beta S RBD mutations did not significantly alter binding affinity for ACE2, despite the presence of N501Y and E484K mutations. Consequently, we tested how the single K417N impacted S binding to ACE2 in a similar manner. Notably, there is a significant decrease in S binding affinity for ACE2 when the K417N mutation is introduced (**Figure 3.3B&C**). Upon further structural analysis, K417, which is located within an integral structural loop, interacts directly with ACE2, and is no longer able to interact with D30 of ACE2 (**Figure 3.3A**). Furthermore, the N501Y and E484K mutations in SARS-CoV-2 Beta variant energetically offset the unfavorable K417N mutation and potentially impact binding affinity in a similar manner in Gamma (P.1) containing the K417T mutation (**Figure 3.2 B&C).**

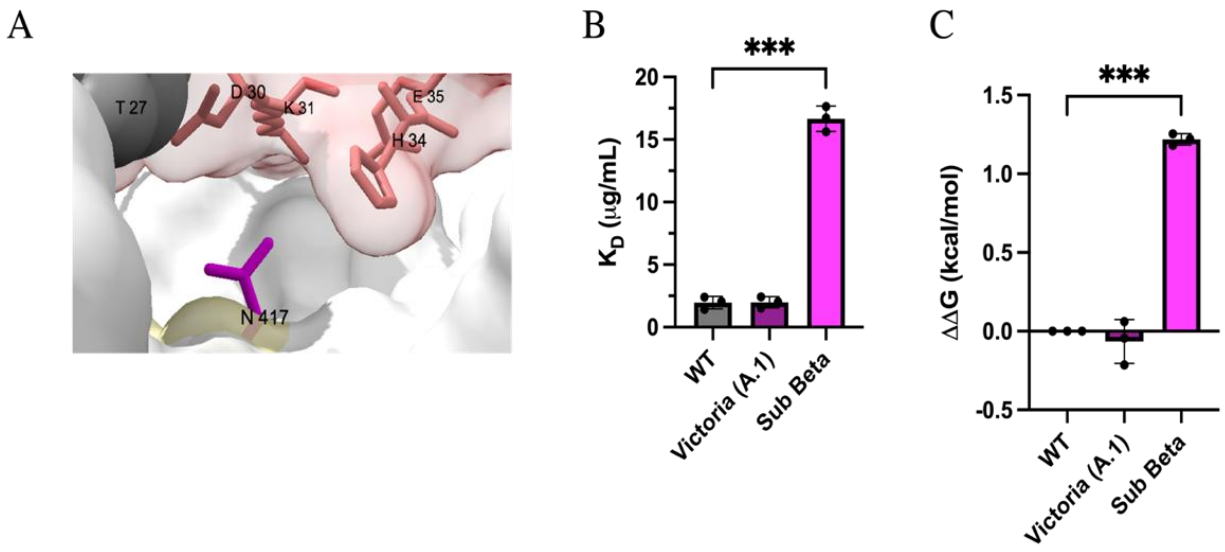

Figure 3.3 (A) S K417N (magenta) within ACE2 interaction site (yellow) and ACE2 interacting amino acid residues (salmon) (PDB:7KJ2). (B) Dissociation constants (K_d) and (B) relative binding energy of S RBD point mutations of SARS-CoV-2 variants binding affinity ACE2 WT using $\Delta\Delta G = RT\ln(K_d/K_{d\ \text{Spike WT}})$ * $p<0.05$, ** $p<0.005$, *** $p<0.0005$ for Dunnett's multiple comparisons test.

Table 3.1: Effect of Spike point mutations on K_d binding ACE2 WT by BLI.

SARS-CoV-2 Variant	Spike mutations[a]	K_d[b]	Gibbs Free Energy[c]	Relative Binding Free Energy[d]
Victoria (A.1)	WT(D614G)	1.99 ± 0.18	7.88 ± 0.06	0.00 ± 0.06
Alpha (B.1.17)	N501Y	0.81 ± 0.19[e]	8.43 ± 0.15	-0.55 ± 0.15
Beta (B.1.351)	N501Y/E484K/K417N	1.35 ± 0.02	8.10 ± 0.01	-0.23 ± 0.01
Sub Beta	K417N	16.67 ± 1.02[f]	6.60 ± 0.04	1.27 ± 0.04
Gamma (P.1)	N501Y/E484K/K417T	1.60 ± 0.19	8.01± 0.07	-0.14 ± 0.07
Zeta (P.2)	E484K	0.68 ± 0.35[f]	8.52 ± 0.35	-0.64 ± 0.35
Theta (P.3)	N501Y/E484K	0.52 ± 0.13[f]	8.68 ± 0.16	-0.80 ± 0.16
Epsilon (B.1.429)	L452R	1.82 ± 0.25	7.93 ± 0.08	-0.06 ± 0.08
Iota (B.1.526)	E484K/S477N	0.75 ± 0.27[f]	8.46 ± 0.21	-0.58 ± 0.21
Delta/Kappa (B.1.617)	E484Q/L452R	0.89 ± 0.36[e]	8.36 ± 0.29	-0.49 ± 0.29

[a]Expressed in HEK293 cells. [b]Average values (μg/mL) ± one standard deviation (n=3). [c]ln kcal/mol, from $\Delta G = -RT\ln(K_d)$. [d]ln kcal/mol, from $\Delta\Delta G = RT\ln(K_{d1}/K_{SpikeWT})$. [e]$p < 0.005$. [f]$p < 0.0005$.

DISCUSSION

The results described in this report demonstrate the selective pressure that drives viral mutagenesis for enhanced binding to the host cell receptor. It is crucial to fully understand how S RBD mutations within SARS-CoV-2 variants promote viral replication.

Here, we compare the binding affinity of S RBD mutations associated with SARS-CoV-2 variant strains for soluble human ACE2 host cell receptor using BLI. Our results attribute changes in binding affinity values to individual S RBD mutations present in SARS-CoV-2 variants. The biophysical quantities can be detected by BLI and applied to the observed structural changes within the S trimer.

Our results show that S RBD variants containing N501Y and E484K/Q mutations are favorable for ACE2 binding compared to S wildtype, apart from Alpha and Gamma variants. Interestingly, we calculated a positive relative binding energy for the K417N mutation that is present in the Beta variant and is unfavorable for ACE2 binding. However, we note that these relative binding energies are additive and offset the unfavorable mutation. This result attests to the structural modifications the S RBD undergoes to stabilize binding to ACE2.

Though there are other reported binding affinities for S RBD mutations[5, 7, 48, 49], previous studies only analyze interactions with the RBD[11]. Our study is unique in that we limited glycosylation to oligomannose expression to achieve uniform N-glycan processing for both S and ACE2. Additionally, we analyze the interaction between trimeric S and ACE2 monomers, which may alter the kinetics of the S-ACE2 interaction compared to ACE2 interactions with S-RBD.

The data reported here provides context for the molecular features that guide viral mutagenesis that could potentially be used to predict other mutated regions of S. Consequently, this prediction could be utilized to design more potent therapeutics or vaccines for emerging strains of SARS-CoV-2. Additional future studies may include quantification of binding affinities with Spike trimer purified from pseudoviruses and patient-derived SARS-CoV-2 virions.

METHODS

Generation of Expression Constructs Encoding Wild Type and Mutant Forms of Spike and ACE2:

Expression constructs for mutant forms of Spike (D614G, D614G/N501Y, D614G/E484K, D614G/K417N, D614G/N501Y/E484K, D614G/L452R, D614G/N501Y/E484K/K417N, D614G/N501Y/E484K/K417T, D614G/E484K/S477N and D614G/E484Q/L452R) were generated using New England BioLabs Q5 Mutagenesis Kit (cat#0554S). The primers for each mutation were designed using NEBaseChanger program (https://nebasechanger.neb.com) and plasmid DNA preparations were generated for expression in HEK293S (GnTI-) cells (ATCC).

Expression and Purification Spike and ACE2:

Wild type and mutant forms of Spike and ACE2 proteins were, kindly provided by the Moremen and Wells lab, expressed as soluble secreted proteins by transient transfection of suspension cultures in HEK293S (GnTI-) cells maintained at 0.5–3.0x10^6 cells/ml in a humidified CO_2

platform shaker incubator at 37°C with 50% humidity and 125 rpm. Transient transfection was performed at a cell density of 2.5-3.0x10^6 cells/ml in expression medium comprised of a 9:1 ratio of Freestyle^{TM}293 expression medium (Thermo Fisher Scientific, Waltham MA) and EX-Cell expression medium including Glutmax (Sigma-Aldrich). Transfection was initiated by the addition of plasmid DNA and polyethyleneimine as transfection reagent (linear 25-kDa polyethyleneimine, Polysciences, Inc., Warrington, PA). Cell cultures were diluted with an equal volume of fresh media supplemented with valproic acid (2.2 mM final concentration) twenty-four hours post-transfection and protein production was continued for an additional 5 days at 37°C, 5% CO_2 with 125 rpm shaking. Cell cultures were harvested, clarified by sequential centrifugation at 1200 rpm for 10 min and 3500 rpm for 15 min at 4°C, and passed through a 0.8 μM filter (Millipore, Billerica, MA). The protein preparations were adjusted to contain 20 mM HEPES, 20 mM imidazole, 300 mM NaCl, pH 7.5, and subjected to Ni-NTA Superflow (Qiagen, Valencia, CA) chromatography using a column pre- equilibrated with Buffer I (20 mM HEPES, 300 mM NaCl, 20 mM imidazole, pH 7.5). The sample was loaded onto the column, washed with 3 column volumes of Buffer I, washed with 3 column volumes of Buffer II (20 mM HEPES, 300 mM NaCl, 50 mM imidazole) and eluted with Elution Buffer (20 mM HEPES, 300 mM NaCl, 300 mM imidazole, pH 7.0). The elution sample was concentrated using a 10 kDa molecular mass cut-off ultrafiltration pressure cell (Millipore, Billerica, MA). Purified Spike and ACE2 proteins from HEK293S (GnTI-) was added to a Superdex G-200 gel filtration column (GE Healthcare) pre-equilibrated and eluted with Gel Filtration Buffer (20 mM HEPES, 100 mM NaCl, 0.05% sodium azide, pH 7.0) The eluted protein was stored at 4°C or 20°C. Prior to use

the protein was thawed on ice and centrifuged at 8000 rcf for 20 minutes and supernatant was collected.

Biolayer Interferometry Binding Assays:

Spike (WT or mutants) were immobilized onto amine reactive "second-generation" biosensors (AR2G, Cat#: 18-5092, Pall ForteBio Corp., Menlo Park, CA, USA) by activation with 20mM EDC and 10mM sulfo-NHS solution for 1800s. Spike (20 μg/mL) was coupled to biosensors for 1800s, followed by quenching in 1M ethanolamine (pH8.5) for 600s. The immobilization resulted in a loading signal of approximately 1.5 nm.

Binding experiments were performed in PBST buffer (1xPBS with 0.1% Tween-20 at pH7.4, at 25°C), EDC (1-ethyl-3-(3-dimethylaminopropyl)carbodiimide hydrochloride Prod# 22980, Thermo Scientific, Rockford, IL, USA), Sulfo-NHS (Sulfo-NHS (N-hydroxysulfosuccinimide), Prod#24510, Thermo Scientific, Rockford, IL, USA), 10xPBS (10x Phosphate Buffered Saline, Cat#:1610780, Bio-Rad, Hercules, CA, USA), Ethanolamine (Cat# 110167, Sigma- Aldrich, St. Louis, MO, USA), Amine Reactive Second Generation biosensors (AR2G, Cat#: 18-5092, Pall ForteBio Corp., Menlo Park, CA, USA).

Direct binding constants (K_d) were measured using a BioLayer Interferometer (BLI) Octet Red 384 system (Pall ForteBio Corp., Menlo Park, CA, USA) and data was acquired using ForteBio Data Acquisition 8.2 software (Pall ForteBio Corp., Menlo Park, CA, USA). A baseline reading was collected for 120s in PBST Buffer only; then, both association and dissociation responses were detected for 600s. ACE2 wild type sample was prepared in two- fold serial dilution in

PBST from 0 to 80 μg/mL, and binding recorded in triplicate. S mutants that showed tighter binding were assayed with a concentration range of 0 to 20 μg/mL ACE2 to obtain a more linear fit. Binding constants were calculated using Prism 10 (GraphPad Prism, USA) assuming a site-specific 1:1 binding model.

CHAPTER 4

THE ROLE OF SARS-COV-2 SPIKE EVOLUTION ON THE EFFICACY OF ANTI-SPIKE MONOCLONAL ANTIBODIES

INTRODUCTION

Coronavirus Disease 19 (COVID-19) that is caused by severe acute respiratory syndrome coronavirus-2 (SARS-CoV-2) resulted in a global pandemic due to the fatality and transmission rate. The initial step of infection is the interaction between the Spike (S) glycoprotein and its human angiotensin-converting enzyme 2 (ACE2) receptor. As a result, emergency therapeutics such as monoclonal antibodies (mAbs) were designed to inhibit the S-ACE2 interaction. Although vaccines and host adaptive immunity reduced the severity of COVID-19, antigenic drift drives S mutations across variants[4, 6, 8, 36]. Specifically, the S receptor binding domain (RBD) of SARS-CoV-2 variants display a rapid rate of mutations[4, 6, 8, 36]. Thus, the need to understand how current anti-S mAbs interact with S RBD mutations is essential for more effective COVID-19 treatment.

Monoclonal antibodies are proteins derived from a single B-cell that are designed to target a specific epitope on an antigen[50, 51]. They are a powerful diagnostic and therapeutic across various diseases due to their high specificity. SARS-CoV-2 therapeutic mAbs mainly target the S protein[50-52]. The most common target epitope is the RBD of S to physically block binding the ACE2 receptor[45, 50-53]. However, the rapid accumulation of mutations in the S RBD in emerging SARS-

CoV-2 variants presents challenges for mAb efficacy. Previous viral neutralization assays display immune escape and reduced binding of mAbs of SARS-CoV-2 variants with dominant RBD mutations, pointedly those associated with increased ACE2 binding (**Table 4.1**)[12, 23, 54-56]. Thus, it is important to understand the interaction between SARS-CoV-2 and mAbs and the molecular properties that mediate their interaction for the design of novel mAbs with increased efficacy.

Glycosylation and RBD mutations often are not mutually exclusive and can have synergistic effects on immune evasions[31, 38, 57]. Emerging strains of SARS-CoV-2 gain many mutations within the S RBD that contribute to changes in ACE2 interactions and conformational dynamics[5, 11, 26, 33, 58, 59]. For example, more recent biophysical analyses indicate that Omicron (BA.1) S trimer only presents in a single-up conformation to retain a prolonged monovalent binding to ACE2 while minimizing RBD exposure for reduced mAb recognition[27, 37]. Furthermore, SARS-CoV-2 strains display modified S glycan binding dynamics with ACE2[38, 39], suggesting mutations in BA.1 S RBD precludes unfavorable interactions with ACE2 glycans. However, it is not well understood how ACE2 N-glycan mutations affect mAb binding affinity for S, and consequently, their potency in select human individuals.

To explore how ACE2 N-glycan variants may influence mAb recognition of the S glycoprotein, we performed structural analyses to investigate protein-glycan molecular interactions. SARS-CoV-2 S sequence and structural alignments display overlapping interactions sites made by current SARS-CoV-2 therapeutic mAbs and ACE2 glycans N90, N322, and N546 (**Figure 4.2A&B**). To further investigate these observations, we performed a competition assay to evaluate S-CR3022 inhibiting binding to ACE2 wildtype and N-glycan mutants. Together, these

results describe the energetic impact on S-mAb interaction and provide insights for future anti-Spike therapeutic design.

Table 4.1: Summary of SARS-CoV-2 variant RBD mutations involved in immune escape.

Mutation	Associated Variant(s) (Examples)	Effect on mAb Binding / Neutralization
K417N/T	Beta (B.1.351), Gamma (P.1), Omicron (B.1.1.529)	Reduces binding/neutralization by Class 1 antibodies (e.g., those targeting the ACE2-binding ridge)[12, 54, 55].
E484K	Beta (B.1.351), Gamma (P.1), Omicron (B.1.1.529), Iota (B.1.526)	Hotspot for escape; significantly reduces binding/neutralization by Class 2 antibodies (often those targeting the receptor-binding motif). Can also reduce convalescent plasma neutralization[12, 54-56].
L452R	Delta (B.1.617.2), Epsilon (B.1.427/B.1.429), Omicron subvariants (e.g., some XBB)	Reduces binding/neutralization by certain Class 3 antibodies. Often associated with increased transmissibility[12, 23, 55].
S477N	Iota (B.1.526, Omicron (BA.1-BA.5, XXB, JN.1)	Can reduce binding of some RBD-targeting antibodies. Often co-occurs with other escape mutations[12, 54].

RESULTS

S RBD variants expressing the N501Y/E484K or E484Q/L452R mutations are unfavorable for CR3022 binding affinity.

CR3022 is a mAb isolated from a SARS-CoV patient that was used as a framework for current anti-S mAbs to treat SARS-CoV-2[60]. Here, we use BLI based binding assays to quantify the energetic contributions of individual S RBD mutations associated with SARS-CoV-2 variants

binding to CR3022. Our results reveal that S RBD variants expressing N501Y/E484K or E484Q/L452R mutations decrease CR3022 binding to S (**Figure 4.2C**), which is the opposite result of enhanced S binding affinity for ACE2. However, the mutations display a similar additive pattern as S binding affinity for ACE2 is altered and supports our experimental design to quantify the magnitude of individual mutations on binding affinity using BLI. Thus, our results demonstrate how viral evolution is driven by selective pressures and provides a construct to evaluate and predict future SARS-CoV-2 variants.

N-glycans N74 and N165 play a role in stabilizing and exposing the S RBD for CR3022 mAb binding.

Prior binding studies implicate that N165 plays a role in stabilizing the open conformation and presenting the S RBD for ACE2 binding[57]. However, our binding assays with S-ACE2 support that both N165 and N74 significantly improve the open conformation for ACE2 binding. On the basis that CR3022 is only able to bind S in its open conformation, we quantified CR3022 binding affinity for S N165Q/N74K, which showed an approximate two-fold reduction in binding affinity (**Figure 4.1B**). Thus, this result further supports the role that N165 and N74 glycans play in exposing and stabilizing the S RBD.

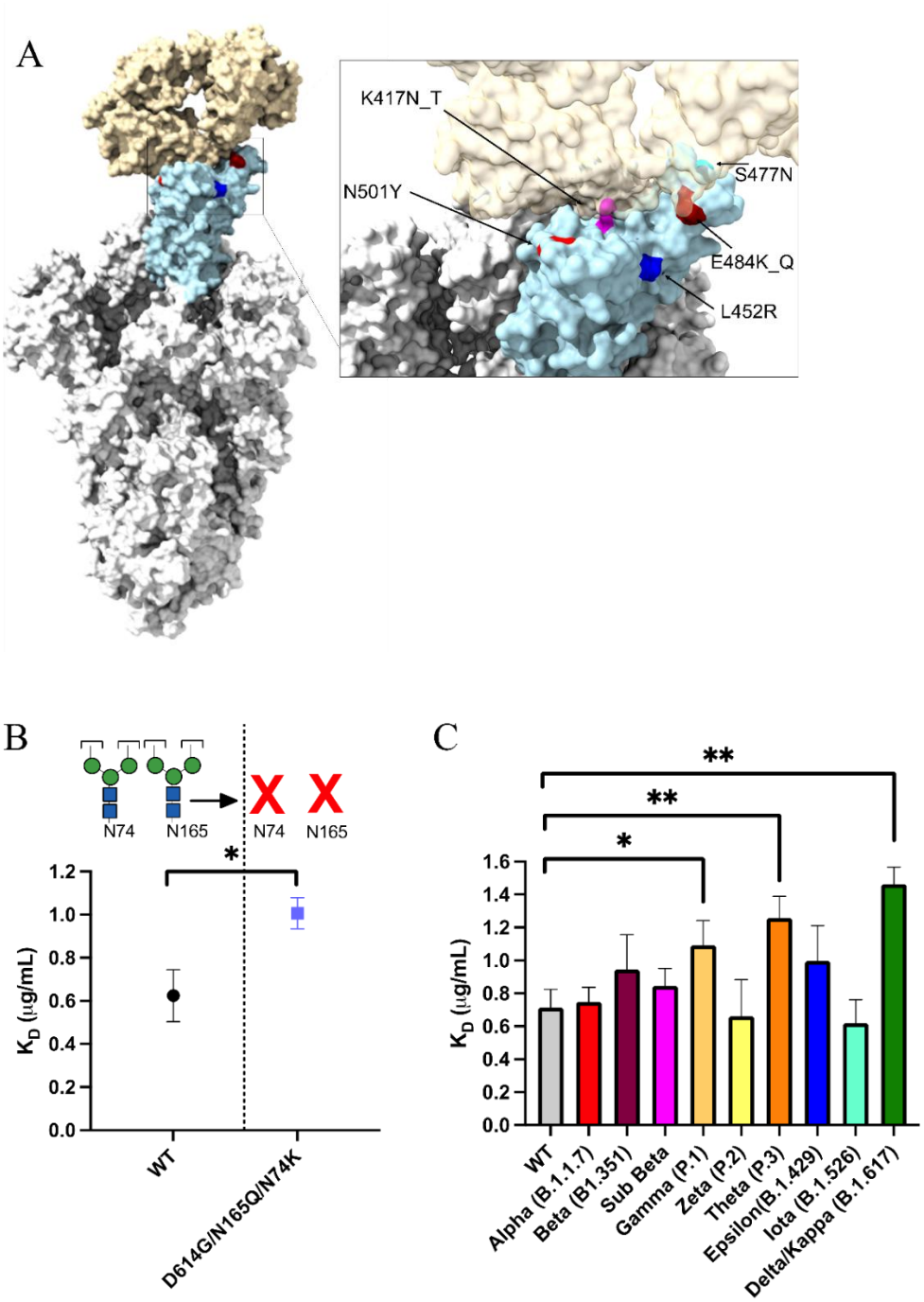

Figure 4.1 (A) Spike trimer (white) of SARS-CoV-2, RBD (light blue) point mutations N501Y (red), K417N_T (magenta), L452R (blue), E484K_Q (dark red), S477N (cyan) bound to CR3022 (wheat) (PDB:7KJ2, 6YOR superimposed model). (B) Dissociation constants (K_d) of S wildtype

and S N165Q/N74K N-glycan mutant. (C) Dissociation constants (K_d) of S wildtype and S RBD point mutations of SARS-CoV-2 variants binding affinity ACE2 WT * p<0.05, ** p<0.005, *** p<0.005, Dunnett's multiple comparisons test relative to Spike WT.

Table 4.2: Effect of Spike point mutations on K_d binding CR3022 by BLI.

SARS-CoV-2 Variant	Spike mutations[a]	K_d[b]	Fold Change	Relative Binding Free Energy[c]
Victoria (A.1)	WT(D614G)	0.60 ± 0.10	1.0	0.00 ± 0.11
Alpha (B.1.17)	N501Y	0.68 ± 0.07	1.1	0.07 ± 0.06
Beta (B.1.351)	N501Y/E484K/K417N	0.95 ± 0.02[e]	1.6	0.28 ± 0.01
Sub Beta	K417N	0.73 ± 0.05	1.2	0.11 ± 0.04
Gamma (P.1)	N501Y/E484K/K417T	1.09 ± 0.11[e]	1.8	0.36 ± 0.06
Zeta (P.2)	E484K	0.92 ± 0.12[d]	1.5	0.25 ± 0.08
Theta (P.3)	N501Y/E484K	1.23 ± 0.10[e]	2.1	0.43 ± 0.05
Epsilon (B.1.429)	L452R	0.81 ± 0.18	1.4	0.17 ± 0.13
Iota (B.1.526)	E484K/S477N	0.76 ± 0.08	1.3	0.13 ± 0.07
Delta/Kappa (B.1.617)	E484Q/L452R	1.60 ± 0.19[e]	2.6	0.59 ± 0.07

[a]Expressed in HEK293 cells. [b]Average values (μg/mL) ± one standard deviation (n=3). [c]ln kcal/mol, from $\Delta\Delta G = RT\ln(K_{d1}/K_{d2})$. [d]$p < 0.05$. [e]$p < 0.005$.

ACE2 N-glycans influence CR3022 inhibition of S due to altered S N165 and N74 glycan interaction with ACE2 and ACE2 N-glycans.

Our previous binding studies show that S N165 and N74 glycan removal significantly decreases binding affinity for ACE2 and CR3022 mAb. These results agree with the hypothesis that S N165 and N74 glycans make crucial contacts to support the S trimer in the "open" conformation to expose the RBD for enhanced binding[33, 43, 60]. To further observe how S N165 and N74 glycans interact with ACE2 and CR3022, we employed a competition assay with ACE2 N-glycan mutants.

Here, we observed an enhanced binding of ACE2 N90S and ACE2 N322S to S-CR3022 complex, which indicates that ACE2 N90 and N322 glycans are favorable in CR3022 blocking S WT (**Figure 4.2B, Table 4.2**). Notably, ACE2 N90S is a ACE2 genetic variant in the human population[14], which may serve as a factor influencing severity of SARS-CoV-2 infection. When comparing S WT to S N74K/N165Q, we do not observe altered binding except for decreased CR3022 blocking for ACE2 N322S (**Figure 4.2B, Table 4.2**). This result indicates that N322 glycan does perform some S-shielding, but S N74 and N165 form inter-glycan interactions to for further exposure of S RBD and has been previously observed by structural analyses[33, 34, 47]. Thus, S N-glycosylation and ACE2 N-glycosylation influence CR3022 ability to block S-ACE2 binding.

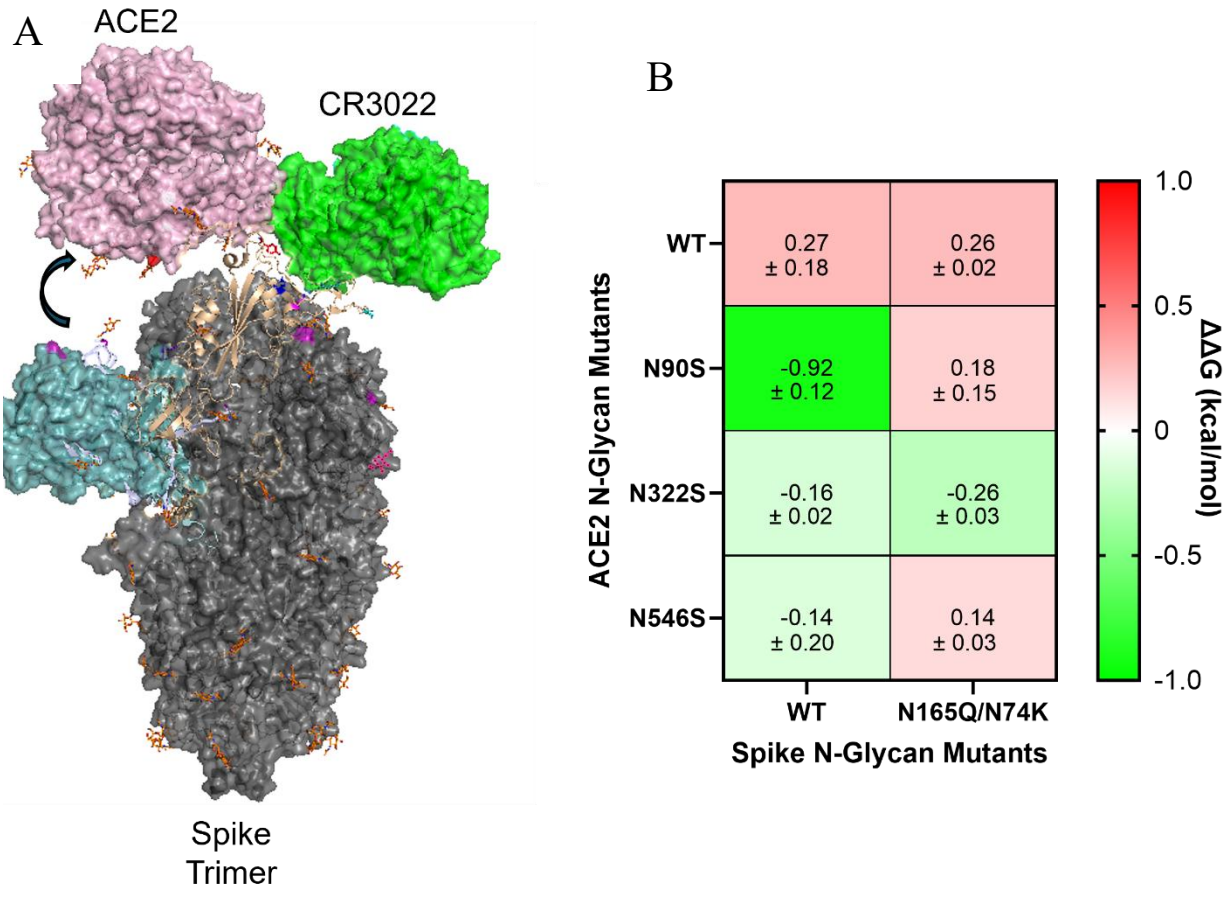

Figure 4.2 (A) Spike trimer (dark gray) binding ACE2 (pink) (PDB:7KJ2) superimposed with S-RBD (wheat)-CR3022 (green) (PDB:6YOR). (B) Relative binding energy of S RBD point mutations of SARS-CoV-2 variants incubated with and without CR3022 mAb binding affinity ACE2 WT and N-glycan mutants using $\Delta\Delta G = RT\ln (K_{d\ mAb+ACE2}/K_{d\ ACE2})$.

Table 4.3: Effect of CR3022 Spike N74K/N165Q blocking ACE2 in relative binding energy by BLI.

ACE2 mutations[a]	Spike WT[a,b]	Spike N74K/N1655Q[a,b]
WT	0.27 ± 0.18	0.26 ± 0.02
N90S	-0.92 ± 0.12[e]	0.18 ± 0.15
N322S	-0.16 ± 0.02[d]	-0.26 ± 0.03[d]
N546S	-0.14 ± 0.20	0.14 ± 0.03

[a]Expressed in HEK293 cells. [b]Average [c]ln kcal/mol, from $\Delta\Delta G = RT\ln(K_{d1}/K_{d2})$ ± one standard deviation (n=3). [d]$p < 0.05$. [e]$p < 0.005$.

ACE2 N-glycans influence CR3022 inhibition of S due to altered S RBD mutations with ACE2 N-glycans.

Based on our previous structural analyses, we observed overlapping contact sites on S RBD by both CR3022 and ACE2 and ACE2 N-glycans that coordinate with mutations identified in SARS-CoV-2 variants (**Figure 4.4B**). Therefore, we aimed to reveal how such S RBD mutations and ACE2 N-glycan mutations would influence mAb inhibition of S binding. Interestingly, our data showed that individual removal of ACE2 N90, N322, or N546 variably alters mAb binding affinity for S RBD VOC mutations suggesting ACE2 N-glycans could potentially influence mAb-S neutralization. The blocking assay revealed that S wildtype blocks S wildtype interaction with ACE2 wildtype (**Figure 4.4A**). For ACE2 wildtype and N90S blocking, the K417N mutation

appears to improve CR3022 binding affinity for S; however, it may be that the N90 glycan stabilizes the K417N mutation on S (**Figure 4.4B**). However, ACE2 N90S, N322, and N546 appear to outcompete CR3022 for S wildtype (**Figure 4.4A-D**), which agrees with our earlier study that the ACE2 N-glycosylation significantly reduces S binding affinity and may also cause clashing with antibody (**Figure 4.2A**). Notably, there is little change when ACE2 N322S, indicating it does not greatly affect CR3022 binding and agrees with the structural analyses (**Figure 4.4 A-B & Figure 4.4C**). Further, most of the S RBD mutations move toward no change in binding with the presence of CR3022, apart from K417N. Yet, the S E484K mutation with ACE2 N546S blocking resulted in increased CR3022 blocking (**Figure 4.4D**). This potentially could result in altered N-glycan interactions and less steric hinderance with the N546 removal; however, additional structural analyses should be performed to determine the N-glycan interactions. Collectively, the results reported by the ACE2 blocking assays provide insight into how ACE2 polymorphisms could affect mAb potency and the molecular features that should be considered for future therapeutic mAb design.

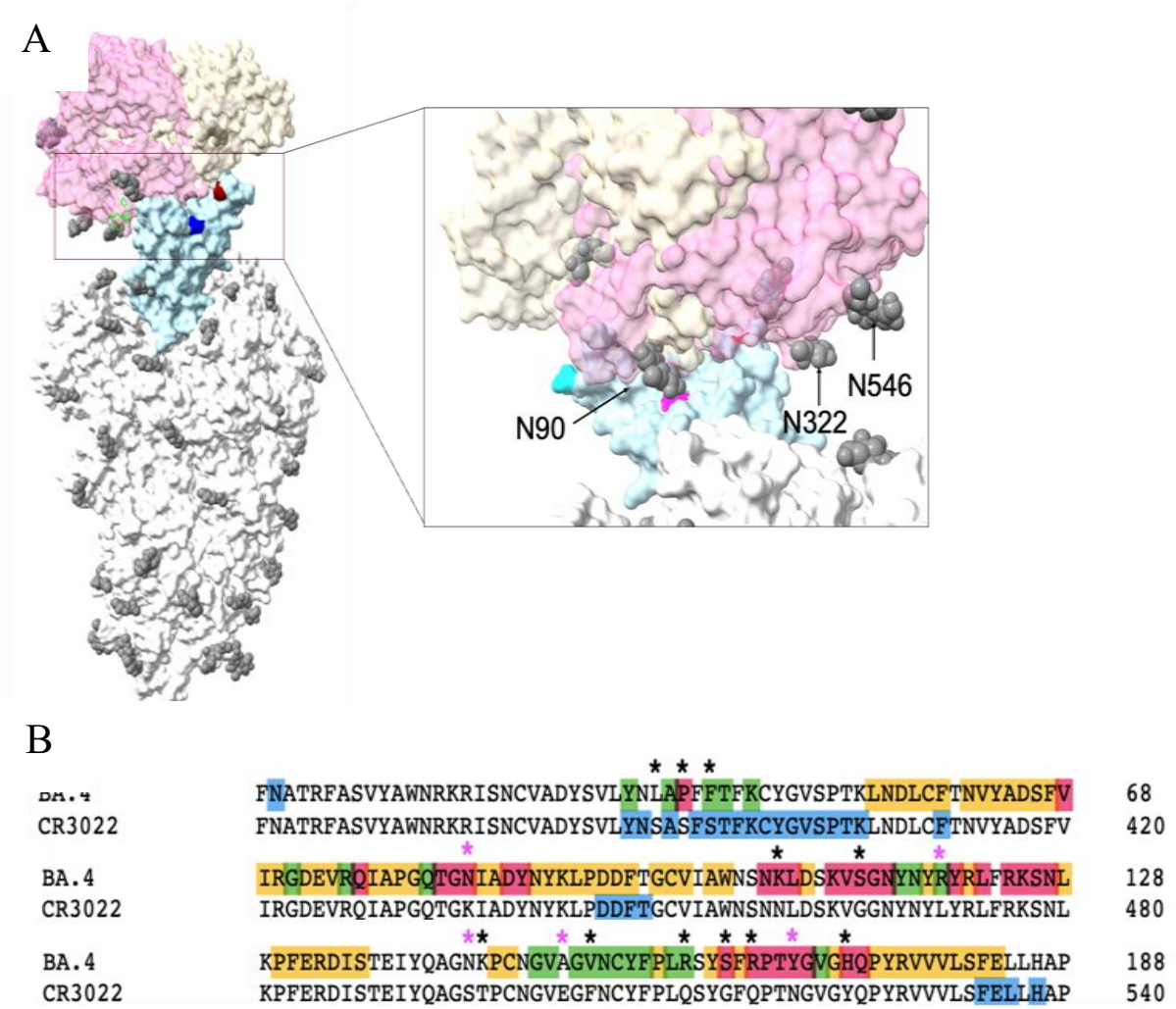

Figure 4.3 (A) Spike trimer (white) of SARS-CoV-2, RBD (light blue) point mutations N501Y (red), K417N_T (magenta), L452R (blue), E484K_Q (dark red), S477N (cyan) bound to CR3022 (wheat) (PDB:7KJ2, 6YOR superimposed model). (B) Sequence alignment of S RBD our mutations (pink asterisks) and Omicron (BA.4) (black asterisks) with highlighted contact sites for ACE2 (yellow), ACE2 N90 (red), ACE2 N322 (green)

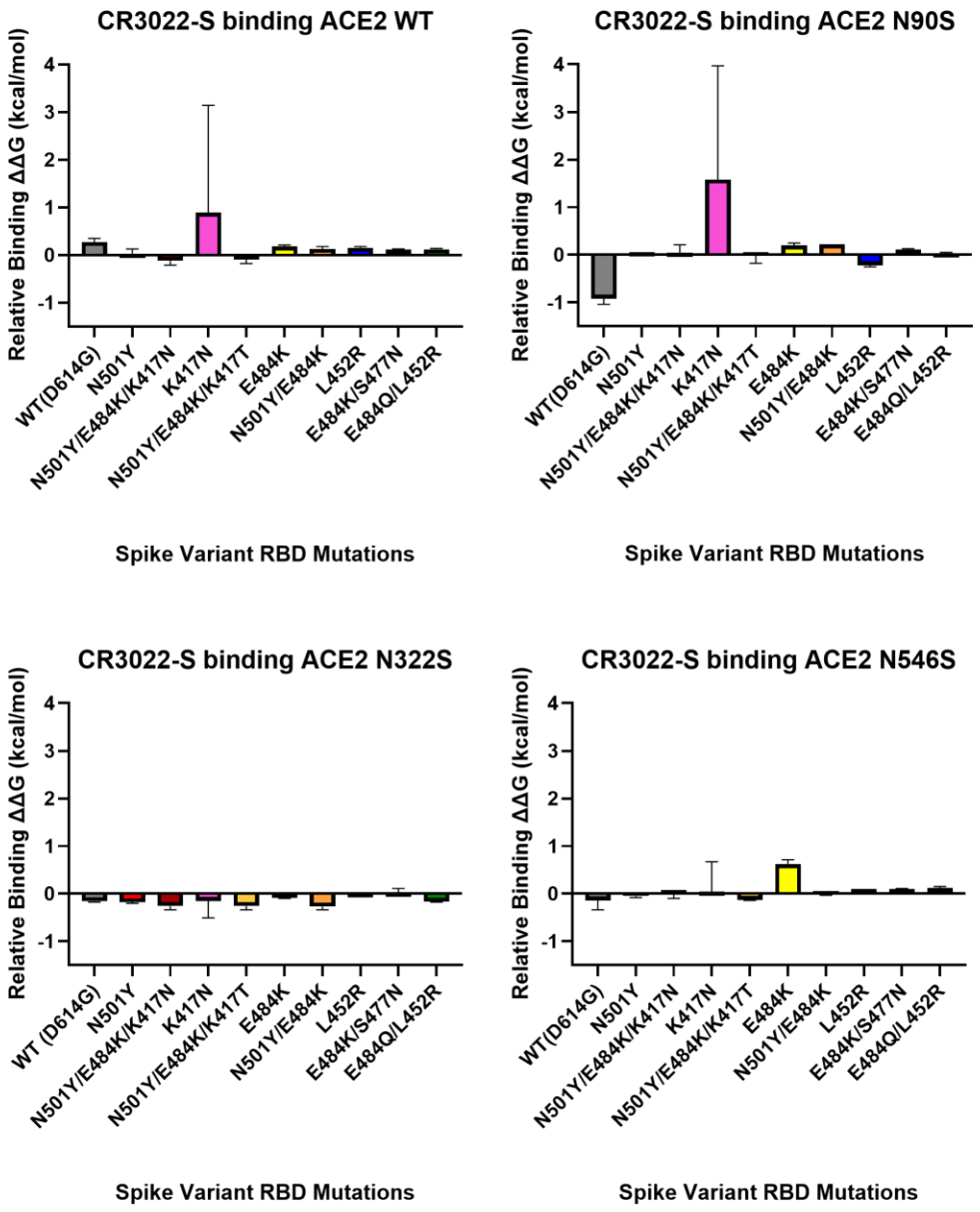

Figure 4.4 (A-D) Relative binding energy of S RBD point mutations of SARS-CoV-2 variants incubated with and without CR3022 mAb binding affinity ACE2 WT and N-glycan mutants using $\Delta\Delta G = RT\ln (K_{d\ mAb+ACE2}/K_{d\ ACE2})$.

Table 4.4: Effect of Spike-CR3022 point mutations on K_d binding ACE2 point mutations by BLI.

ACE2 mutations[a]	SARS-CoV-2 Variant	Spike mutations[a]	Relative Binding Free Energy[c]
WT	Victoria (A.1)	WT(D614G)	0.27 ± 0.08
	Alpha (B.1.17)	N501Y	0.02 ± 0.11
	Beta (B.1.351)	N501Y/E484K/K417N	-0.12 ± 0.09
	Sub Beta	K417N	0.89 ± 2.25
	Gamma (P.1)	N501Y/E484K/K417T	-0.09 ± 0.09[d]
	Zeta (P.2)	E484K	0.18 ± 0.03
	Theta (P.3)	N501Y/E484K	0.13 ± 0.05
	Epsilon (B.1.429)	L452R	0.15 ± 0.03
	Iota (B.1.526)	E484K/S477N	0.11 ± 0.02
	Delta/Kappa (B.1.617)	E484Q/L452R	0.12 ± 0.02
N90S	Victoria (A.1)	WT(D614G)	-0.92 ± 0.12[d]
	Alpha (B.1.17)	N501Y	0.05 ± 0.00
	Beta (B.1.351)	N501Y/E484K/K417N	0.04 ± 0.17
	Sub Beta	K417N	1.58 ± 2.39
	Gamma (P.1)	N501Y/E484K/K417T	-0.02 ± 0.16
	Zeta (P.2)	E484K	0.20 ± 0.05
	Theta (P.3)	N501Y/E484K	0.22 ± 0.00
	Epsilon (B.1.429)	L452R	-0.22 ± 0.03[d]

	Iota (B.1.526)	E484K/S477N	0.11 ± 0.02
	Delta/Kappa (B.1.617)	E484Q/L452R	0.03 ± 0.02
	Victoria (A.1)	WT(D614G)	-0.16 ± 0.02[d]
	Alpha (B.1.17)	N501Y	-0.18 ± 0.02[d]
	Beta (B.1.351)	N501Y/E484K/K417N	-0.26 ± 0.08[d]
	Sub Beta	K417N	-0.15 ± 0.36
N322S	Gamma (P.1)	N501Y/E484K/K417T	-0.26 ± 0.08[d]
	Zeta (P.2)	E484K	-0.09 ± 0.01[d]
	Theta (P.3)	N501Y/E484K	-0.27 ± 0.07[d]
	Epsilon (B.1.429)	L452R	-0.08 ± 0.00[d]
	Iota (B.1.526)	E484K/S477N	0.02 ± 0.09
	Delta/Kappa (B.1.617)	E484Q/L452R	-0.17 ± 0.01[d]
	Victoria (A.1)	WT(D614G)	-0.14 ± 0.20
	Alpha (B.1.17)	N501Y	-0.05 ± 0.03[d]
	Beta (B.1.351)	N501Y/E484K/K417N	-0.01 ± 0.09[d]
	Sub Beta	K417N	0.04 ± 0.63
N546S	Gamma (P.1)	N501Y/E484K/K417T	-0.13 ± 0.01[d]
	Zeta (P.2)	E484K	0.62 ± 0.09[d]
	Theta (P.3)	N501Y/E484K	-0.02 ± 0.01[d]
	Epsilon (B.1.429)	L452R	0.10 ± 0.00
	Iota (B.1.526)	E484K/S477N	0.10 ± 0.01
	Delta/Kappa (B.1.617)	E484Q/L452R	0.12 ± 0.03

[a]Expressed in HEK293 cells. [b]Average [c]ln kcal/mol, from $\Delta\Delta G = RT\ln(K_{d1}/K_{d2})$ ± one standard deviation (n=3). [d]$p < 0.05$.

DISCUSSION

The SARS-CoV-2 S RBD is recognized as a prominent therapeutic target due to the crucial role in binding ACE2 host receptor for cell adhesion during infection. Monoclonal antibodies (mAbs) were one of the first lines of treatment for those with severe SARS-CoV-2 infection due to their specificity for their target, and reduced likelihood of causing severe side effects. However, the S RBD has gained many mutations across SARS-CoV-2 variants[4, 6, 8, 36], which makes it a challenge to design potent novel mAbs and vaccines[4, 6, 8, 36]. Thus, the need to understand how current anti-S mAbs interact with mutated S RBDs is essential for more effective COVID-19 treatment.

Here, our results demonstrate how S RBD mutations observed in SARS-CoV-2 variants and N-glycosylation mediate CR3022 mAb inhibition. In direct binding assays, we used BLI to calculate equilibrium based direct binding constants to determine the effect of CR3022 to bind to S RBD mutations in SARS-CoV-2 variants. Our kinetic values align with our structural analyses that N501Y/E484K mutations in S variants contribute unfavorable affinity for CR3022.

While the S trimer can exist in a single-up, double-up, or triple up state and bind three ligands total[25], which suggests ACE2 N-glycans could induce steric hinderance with CR3022 and reduce CR3022 affinity. Previously, we observed that S N74 and N165 glycans promote ACE2 binding and propose that they stabilize to expose the RBD in the open formation. Thus, we confirm

this result by using BLI to evaluate CR3022 binding to S N165Q/N74K mutant. Remarkably, we detected a 2-fold decrease in binding affinity, which supports our hypothesis that S N165 and N74 promote the open conformation for binding to the RBD.

To further explore the effect of the impact of ACE2 N-glycosylation and S RBD mutations, and CR3022 inhibition, we performed a blocking assay with ACE2 and its N-glycan mutants to determine how individuals contains the T92I or N546D ACE2 mutations might affect mAb inhibition. The combined structural analyses and binding assays display the reduced inhibition of CR3022 to S across variants compared to S wildtype. Interestingly, the relative binding for ACE2 N-glycan mutants and S WT align with the data observed in the ACE2 blocking assay and indicate that CR3022 could potentially be hindered from binding S due to the bulky sugars on S and how many ligands S variants occupy. Additionally, these results could provide context for repositioning of ACE2 N-glycans by S mutations during infection. Further studies would need to be performed to confirm our observations.

Collectively, the results reported by the ACE2 blocking assays provide insight in to how ACE2 polymorphisms could affect mAb potency and the use of structure-guided therapeutic mAb engineering. To further this study, repeating the binding assays with quantification of with Spike trimer purified from pseudoviruses and patient-derived SARS-CoV-2 virions or membrane bound ACE2 *in vivo* would reveal if physiological conditions alter the glycosylation on either protein or their interactions. Furthermore, neutralization assays with therapeutic mAbs would be beneficial to give insight on the extent to which the mAb can inhibit virus from infection.

METHODS

Generation of Expression Constructs Encoding Wild Type and Mutant Forms of Spike and ACE2:

Expression constructs for mutant forms of Spike (D614G, D614G/N501Y, D614G/E484K, D614G/K417N, D614G/N501Y/E484K, D614G/L452R, D614G/N501Y/E484K/K417N, D614G/N501Y/E484K/K417T, D614G/E484K/S477N and D614G/E484Q/L452R) were generated using New England BioLabs Q5 Mutagenesis Kit (cat#0554S). The primers for each mutation were designed using NEBaseChanger program (https://nebasechanger.neb.com) and plasmid DNA preparations were generated for expression in HEK293S (GnTI-) cells (ATCC).

Expression and Purification Spike and ACE2:

Wild type and mutant forms of Spike and ACE2 proteins were, kindly provided by the Moremen and Wells lab, expressed as soluble secreted proteins by transient transfection of suspension cultures in HEK293S (GnTI-) cells maintained at 0.5–3.0x10^6 cells/ml in a humidified CO_2 platform shaker incubator at 37°C with 50% humidity and 125 rpm. Transient transfection was performed at a cell density of 2.5-3.0x10^6 cells/ml in expression medium comprised of a 9:1 ratio of Freestyle^{TM}293 expression medium (Thermo Fisher Scientific, Waltham MA) and EX-Cell expression medium including Glutmax (Sigma-Aldrich). Transfection was initiated by the addition of plasmid DNA and polyethyleneimine as transfection reagent (linear 25-kDa polyethyleneimine, Polysciences, Inc., Warrington, PA). Cell cultures were diluted with an equal volume of fresh media supplemented with valproic acid (2.2 mM final concentration) twenty-

four hours post-transfection and protein production was continued for an additional 5 days at 37°C, 5% CO_2 with 125 rpm shaking. Cell cultures were harvested, clarified by sequential centrifugation at 1200 rpm for 10 min and 3500 rpm for 15 min at 4°C, and passed through a 0.8 μM filter (Millipore, Billerica, MA). The protein preparations were adjusted to contain 20 mM HEPES, 20 mM imidazole, 300 mM NaCl, pH 7.5, and subjected to Ni-NTA Superflow (Qiagen, Valencia, CA) chromatography using a column pre- equilibrated with Buffer I (20 mM HEPES, 300 mM NaCl, 20 mM imidazole, pH 7.5). The sample was loaded onto the column, washed with 3 column volumes of Buffer I, washed with 3 column volumes of Buffer II (20 mM HEPES, 300 mM NaCl, 50 mM imidazole) and eluted with Elution Buffer (20 mM HEPES, 300 mM NaCl, 300 mM imidazole, pH 7.0). The elution sample was concentrated using a 10 kDa molecular mass cut-off ultrafiltration pressure cell (Millipore, Billerica, MA). Purified Spike and ACE2 proteins from HEK293S (GnTI-) was added to a Superdex G-200 gel filtration column (GE Healthcare) pre-equilibrated and eluted with Gel Filtration Buffer (20 mM HEPES, 100 mM NaCl, 0.05% sodium azide, pH 7.0) The eluted protein was stored at 4°C or 20°C. Prior to use the protein was thawed on ice and centrifuged at 8000 rcf for 20 minutes and supernatant was collected.

Biolayer Interferometry Binding Assays:

Spike (WT or mutants) were immobilized onto amine reactive "second-generation" biosensors (AR2G, Cat#: 18-5092, Pall ForteBio Corp., Menlo Park, CA, USA) by activation with 20mM EDC and 10mM sulfo-NHS solution for 1800s. Spike (20 μg/mL) was coupled to biosensors for

1800s, followed by quenching in 1M ethanolamine (pH8.5) for 600s. The immobilization resulted in a loading signal of approximately 1.5 nm.

Binding experiments were performed in PBST buffer (1xPBS with 0.1% Tween-20 at pH7.4, at 25°C), EDC (1-ethyl-3-(3-dimethylaminopropyl)carbodiimide hydrochloride Prod# 22980, Thermo Scientific, Rockford, IL, USA), Sulfo-NHS (Sulfo-NHS (N-hydroxysulfosuccinimide), Prod#24510, Thermo Scientific, Rockford, IL, USA), 10xPBS (10x Phosphate Buffered Saline, Cat#:1610780, Bio-Rad, Hercules, CA, USA), Ethanolamine (Cat# 110167, Sigma- Aldrich, St. Louis, MO, USA), Amine Reactive Second Generation biosensors (AR2G, Cat#: 18-5092, Pall ForteBio Corp., Menlo Park, CA, USA), SARS-CoV-2 Spike Protein (CR3022) Human IgG1 mAb (#37475 Cell Signaling Technology).

Direct binding constants (K_d) were measured using a BioLayer Interferometer (BLI) Octet Red 384 system (Pall ForteBio Corp., Menlo Park, CA, USA) and data was acquired using ForteBio Data Acquisition 8.2 software (Pall ForteBio Corp., Menlo Park, CA, USA). A baseline reading was collected for 120s in PBST Buffer only; then, both association and dissociation responses were detected for 600s. CR3022 mAb sample was prepared in two- fold serial dilution in PBST from 0 to 10 μg/mL, and binding recorded in triplicate. Binding constants were calculated using Prism 10 (GraphPad Prism, USA) assuming a site- specific 1:1 binding model.

For mAb competition assays, the S-immobilized biosensors were incubated in 1000 nM mAb for 1800s, then dipped in 0 or 40 μg/mL ACE2. A baseline reading was collected for 120s in PBST Buffer only; then, both association and dissociation responses were detected for 600s. Binding

constants were calculated using ForteBio Data Analysis 8.2 software (Pall ForteBio Corp., Menlo Park, CA, USA) assuming a site- specific 1:1 binding model.

Structural Analyses:

Spike-ACE2 complex (PDB:7KJ2) modeled in ManAc5 N-glycans using Glycam Glycoprotein Builder (https://glycam.org/). Superimposition of S-ACE2 (PDB:7KJ2) superimposed with S-RBD (wheat)-CR3022 (green) (PDB:6YOR) using ChimeraX[61].

CHAPTER 5

CONCLUSIONS AND FUTURE DIRECTIONS

The overall goal of the research described in this dissertation was to quantify the effects of genetic modifications expressed in trimeric Spike of SARS-CoV-2 influence binding to ACE2 as well as binding of S-specific monoclonal antibody. Alternatively, the aim for this project was to reveal the influence of ACE2 N-glycosylation on S binding along with its RBD mutations and its inhibition by CR3022 mAb. The only studies to quantify the individual binding affinities of SARS-CoV-2 variants were only expressed as S RBD mutants with fully glycosylated ACE2[11]. By using structure-guided analyses and biolayer interferometry, we were able to describe the influence N-glycosylation on ACE2 and S and S RBD mutations of SARS-CoV-2 variants on CR3022 in quantifiable values that are energetically balanced across genetic constructs. Thus, the combination of structure and biophysical analyses prove to be useful method to reveal the molecular mechanisms that mediate SARS-CoV-2 infection and immune evasion.

To further the study of these interactions, creating individual N-glycan knockouts in Spike expressed on pseudoviruses and their interactions with membrane bound N-glycan mutant ACE2 proteins would be beneficial to further understand the mechanism by which N-glycosylation could modulate SARS-CoV-2 infection. While it is beneficial to perform *in vitro* kinetic assays, using molecular biology methods would provide insight into what physiological conditions influence the S-ACE2 interaction, such as temperature and pH, as well as in a non-

rigid array (i.e. proteins in lipid bilayers). In a similar manner, such studies can be used to evaluate the efficacy of therapeutic mAbs. This workflow can be used to study other viral glycoproteins and their interactions with the host ligand. Additionally, this method is useful to guide therapeutic design for other pathogens.

Although this project outlines the role of N-glycosylation of SARS-CoV-2 Spike, our study is limited in that S is expressed in HEK293(GnTI-) to inhibit further glycan processing of S. There are many conditions that influence how a glycoprotein is glycosylated, such as primary sequence and oligosaccharide transferase activity limited by steric hinderance. However, it is not well understood how the rate of N-glycosylation processing affects viral replication of S glycoprotein variants of SARS-CoV-2. This study could reveal an additional role for S N-glycans beyond shielding.

To gather further insight on the effects of N-glycosylation on ACE2 and S, neutralization curves for mAbs against pseudoviruses with varying S glycosylation and variant mutation profiles would provide a better understanding of the extend N-glycosylation influences binding affinity and neutralization potency. An additional study of structural analyses via computational modeling with our oligomannose forms and mAb-S complexes would also reveal how glycans and mutations alter contacts and conformational dynamics.

When considering any interaction of glycoproteins, one considers carbohydrate binding proteins. Because SARS-CoV-2 S is highly glycosylated, it most likely exhibits non-specific binding other host carbohydrate binding proteins, such as Siglecs. Siglecs are sialic acid-binding immunoglobulin-like lectins that are differentially expressed in various immune cell types to either activate or inhibit immunological responses[29]. Many Siglecs are inhibitory and release

proinflammatory mediators in response to detection of polysaccharide with terminal sialic acid. Many pathogens are decorated in sialic acids to "mask" from phagocytosis by immune cells[29]. Alternatively, focusing on mAb based therapeutics may promote specificity and less likely to cause rapid mutations by targeting sialic acid instead.

In conclusion, SARS-CoV-2 remains a public health issue to those who are immunocompromised and are genetically redisposed to severe infection, as described in this thesis. As SARS-CoV-2 evolves, more unknown factors arise and there is a continuous need to develop novel treatments for COVID-19. Collectively, these studies would provide insight into how N-glycosylation of SARS-CoV-2 S could be targeted for therapeutics beyond inhibiting ACE2 binding. Alternative therapeutics, such as lectins, could be used to lessen the SARS-CoV-2 rate of mutation by targeting the glycans on S instead.

REFERENCES

1. Organization WH. World Health Organization; 2024 [cited 2025] data.who.int]. Available from: https://data.who.int/dashboards/covid19/more-resources.

2. Prevention CfDCa. Atlanta, GA: U.S. Department of Health and Human Services, CDC: Centers for Disease Control and Prevention. . Available from: https://covid.cdc.gov/covid-data-tracker.

3. Borczuk AC, Yantiss RK. The pathogenesis of coronavirus-19 disease. J Biomed Sci. 2022;29(1):87. Epub 20221026. doi: 10.1186/s12929-022-00872-5. PubMed PMID: 36289507; PMCID: PMC9597981.

4. Harvey WT, Carabelli AM, Jackson B, Gupta RK, Thomson EC, Harrison EM, Ludden C, Reeve R, Rambaut A, Consortium C-GU, Peacock SJ, Robertson DL. SARS-CoV-2 variants, spike mutations and immune escape. Nat Rev Microbiol. 2021;19(7):409-24. Epub 20210601. doi: 10.1038/s41579-021-00573-0. PubMed PMID: 34075212; PMCID: PMC8167834.

5. Barton MI, MacGowan SA, Kutuzov MA, Dushek O, Barton GJ, van der Merwe PA. Effects of common mutations in the SARS-CoV-2 Spike RBD and its ligand, the human ACE2 receptor on binding affinity and kinetics. Elife. 2021;10. Epub 20210826. doi: 10.7554/eLife.70658. PubMed PMID: 34435953; PMCID: PMC8480977.

6. Ding C, He J, Zhang X, Jiang C, Sun Y, Zhang Y, Chen Q, He H, Li W, Xie J, Liu Z, Gao Y. Crucial Mutations of Spike Protein on SARS-CoV-2 Evolved to Variant Strains Escaping Neutralization of Convalescent Plasmas and RBD-Specific Monoclonal Antibodies. Front

Immunol. 2021;12:693775. Epub 20210817. doi: 10.3389/fimmu.2021.693775. PubMed PMID: 34484190; PMCID: PMC8416052.

7. Mannar D, Saville JW, Sun Z, Zhu X, Marti MM, Srivastava SS, Berezuk AM, Zhou S, Tuttle KS, Sobolewski MD, Kim A, Treat BR, Da Silva Castanha PM, Jacobs JL, Barratt-Boyes SM, Mellors JW, Dimitrov DS, Li W, Subramaniam S. SARS-CoV-2 variants of concern: spike protein mutational analysis and epitope for broad neutralization. Nat Commun. 2022;13(1):4696. Epub 20220818. doi: 10.1038/s41467-022-32262-8. PubMed PMID: 35982054; PMCID: PMC9388680.

8. Miotto M, Di Rienzo L, Gosti G, Bo L, Parisi G, Piacentini R, Boffi A, Ruocco G, Milanetti E. Inferring the stabilization effects of SARS-CoV-2 variants on the binding with ACE2 receptor. Commun Biol. 2022;5(1):20221. Epub 20220106. doi: 10.1038/s42003-021-02946-w. PubMed PMID: 34992214; PMCID: PMC8738749.

9. Cao Y, Yisimayi A, Jian F, Song W, Xiao T, Wang L, Du S, Wang J, Li Q, Chen X, Yu Y, Wang P, Zhang Z, Liu P, An R, Hao X, Wang Y, Wang J, Feng R, Sun H, Zhao L, Zhang W, Zhao D, Zheng J, Yu L, Li C, Zhang N, Wang R, Niu X, Yang S, Song X, Chai Y, Hu Y, Shi Y, Zheng L, Li Z, Gu Q, Shao F, Huang W, Jin R, Shen Z, Wang Y, Wang X, Xiao J, Xie XS. BA.2.12.1, BA.4 and BA.5 escape antibodies elicited by Omicron infection. Nature. 2022;608(7923):593-602. Epub 20220617. doi: 10.1038/s41586-022-04980-y. PubMed PMID: 35714668; PMCID: PMC9385493.

10. Han P, Li L, Liu S, Wang Q, Zhang D, Xu Z, Han P, Li X, Peng Q, Su C, Huang B, Li D, Zhang R, Tian M, Fu L, Gao Y, Zhao X, Liu K, Qi J, Gao GF, Wang P. Receptor binding and complex structures of human ACE2 to spike RBD from omicron and delta SARS-CoV-2. Cell.

2022;185(4):630-40 e10. Epub 20220106. doi: 10.1016/j.cell.2022.01.001. PubMed PMID: 35093192; PMCID: PMC8733278.

11. Valerio M, Borges-Araujo L, Melo MN, Lousa D, Soares CM. SARS-CoV-2 variants impact RBD conformational dynamics and ACE2 accessibility. Front Med Technol. 2022;4:1009451. Epub 20221005. doi: 10.3389/fmedt.2022.1009451. PubMed PMID: 36277437; PMCID: PMC9581196.

12. Moulana A, Dupic T, Phillips AM, Chang J, Roffler AA, Greaney AJ, Starr TN, Bloom JD, Desai MM. The landscape of antibody binding affinity in SARS-CoV-2 Omicron BA.1 evolution. Elife. 2023;12. Epub 20230221. doi: 10.7554/eLife.83442. PubMed PMID: 36803543; PMCID: PMC9949795.

13. Mugnai ML, Shin S, Thirumalai D. Entropic contribution of ACE2 glycans to RBD binding. Biophys J. 2023;122(12):2506-17. Epub 20230506. doi: 10.1016/j.bpj.2023.05.003. PubMed PMID: 37149733; PMCID: PMC10162944.

14. Suryamohan K, Diwanji D, Stawiski EW, Gupta R, Miersch S, Liu J, Chen C, Jiang YP, Fellouse FA, Sathirapongsasuti JF, Albers PK, Deepak T, Saberianfar R, Ratan A, Washburn G, Mis M, Santhosh D, Somasekar S, Hiranjith GH, Vargas D, Mohan S, Phalke S, Kuriakose B, Antony A, Ustav M, Jr., Schuster SC, Sidhu S, Junutula JR, Jura N, Seshagiri S. Human ACE2 receptor polymorphisms and altered susceptibility to SARS-CoV-2. Commun Biol. 2021;4(1):475. Epub 20210412. doi: 10.1038/s42003-021-02030-3. PubMed PMID: 33846513; PMCID: PMC8041869.

15. Zhou P, Yang XL, Wang XG, Hu B, Zhang L, Zhang W, Si HR, Zhu Y, Li B, Huang CL, Chen HD, Chen J, Luo Y, Guo H, Jiang RD, Liu MQ, Chen Y, Shen XR, Wang X, Zheng XS,

Zhao K, Chen QJ, Deng F, Liu LL, Yan B, Zhan FX, Wang YY, Xiao GF, Shi ZL. A pneumonia outbreak associated with a new coronavirus of probable bat origin. Nature. 2020;579(7798):270-3. Epub 20200203. doi: 10.1038/s41586-020-2012-7. PubMed PMID: 32015507; PMCID: PMC7095418.

16. Davies NG, Abbott S, Barnard RC, Jarvis CI, Kucharski AJ, Munday JD, Pearson CAB, Russell TW, Tully DC, Washburne AD, Wenseleers T, Gimma A, Waites W, Wong KLM, van Zandvoort K, Silverman JD, Group CC-W, Consortium C-GU, Diaz-Ordaz K, Keogh R, Eggo RM, Funk S, Jit M, Atkins KE, Edmunds WJ. Estimated transmissibility and impact of SARS-CoV-2 lineage B.1.1.7 in England. Science. 2021;372(6538). Epub 20210303. doi: 10.1126/science.abg3055. PubMed PMID: 33658326; PMCID: PMC8128288.

17. Volz E, Mishra S, Chand M, Barrett JC, Johnson R, Geidelberg L, Hinsley WR, Laydon DJ, Dabrera G, O'Toole A, Amato R, Ragonnet-Cronin M, Harrison I, Jackson B, Ariani CV, Boyd O, Loman NJ, McCrone JT, Goncalves S, Jorgensen D, Myers R, Hill V, Jackson DK, Gaythorpe K, Groves N, Sillitoe J, Kwiatkowski DP, consortium C-GU, Flaxman S, Ratmann O, Bhatt S, Hopkins S, Gandy A, Rambaut A, Ferguson NM. Assessing transmissibility of SARS-CoV-2 lineage B.1.1.7 in England. Nature. 2021;593(7858):266-9. Epub 20210325. doi: 10.1038/s41586-021-03470-x. PubMed PMID: 33767447.

18. Liu Y, Liu J, Plante KS, Plante JA, Xie X, Zhang X, Ku Z, An Z, Scharton D, Schindewolf C, Widen SG, Menachery VD, Shi PY, Weaver SC. The N501Y spike substitution enhances SARS-CoV-2 infection and transmission. Nature. 2022;602(7896):294-9. Epub 20211124. doi: 10.1038/s41586-021-04245-0. PubMed PMID: 34818667; PMCID: PMC8900207.

19. Cele S, Gazy I, Jackson L, Hwa SH, Tegally H, Lustig G, Giandhari J, Pillay S, Wilkinson E, Naidoo Y, Karim F, Ganga Y, Khan K, Bernstein M, Balazs AB, Gosnell BI, Hanekom W, Moosa MS, Network for Genomic Surveillance in South A, Team C-K, Lessells RJ, de Oliveira T, Sigal A. Escape of SARS-CoV-2 501Y.V2 from neutralization by convalescent plasma. Nature. 2021;593(7857):142-6. Epub 20210329. doi: 10.1038/s41586-021-03471-w. PubMed PMID: 33780970; PMCID: PMC9867906.

20. Tuekprakhon A, Nutalai R, Dijokaite-Guraliuc A, Zhou D, Ginn HM, Selvaraj M, Liu C, Mentzer AJ, Supasa P, Duyvesteyn HME, Das R, Skelly D, Ritter TG, Amini A, Bibi S, Adele S, Johnson SA, Constantinides B, Webster H, Temperton N, Klenerman P, Barnes E, Dunachie SJ, Crook D, Pollard AJ, Lambe T, Goulder P, Paterson NG, Williams MA, Hall DR, Consortium O, Consortium IC, Fry EE, Huo J, Mongkolsapaya J, Ren J, Stuart DI, Screaton GR. Antibody escape of SARS-CoV-2 Omicron BA.4 and BA.5 from vaccine and BA.1 serum. Cell. 2022;185(14):2422-33 e13. Epub 20220609. doi: 10.1016/j.cell.2022.06.005. PubMed PMID: 35772405; PMCID: PMC9181312.

21. Rueca M, Berno G, Agresta A, Spaziante M, Gruber CEM, Fabeni L, Giombini E, Butera O, Barca A, Scognamiglio P, Girardi E, Maggi F, Valli MB, Vairo F, Sars-Co VLGSSG. Genomic and Epidemiologic Surveillance of SARS-CoV-2 in the Pandemic Period: Sequencing Network of the Lazio Region, Italy. Viruses. 2023;15(11). Epub 20231031. doi: 10.3390/v15112192. PubMed PMID: 38005872; PMCID: PMC10674723.

22. Dejnirattisai W, Zhou D, Supasa P, Liu C, Mentzer AJ, Ginn HM, Zhao Y, Duyvesteyn HME, Tuekprakhon A, Nutalai R, Wang B, Lopez-Camacho C, Slon-Campos J, Walter TS, Skelly D, Costa Clemens SA, Naveca FG, Nascimento V, Nascimento F, Fernandes da Costa C, Resende

PC, Pauvolid-Correa A, Siqueira MM, Dold C, Levin R, Dong T, Pollard AJ, Knight JC, Crook D, Lambe T, Clutterbuck E, Bibi S, Flaxman A, Bittaye M, Belij-Rammerstorfer S, Gilbert SC, Carroll MW, Klenerman P, Barnes E, Dunachie SJ, Paterson NG, Williams MA, Hall DR, Hulswit RJG, Bowden TA, Fry EE, Mongkolsapaya J, Ren J, Stuart DI, Screaton GR. Antibody evasion by the P.1 strain of SARS-CoV-2. Cell. 2021;184(11):2939-54 e9. Epub 20210330. doi: 10.1016/j.cell.2021.03.055. PubMed PMID: 33852911; PMCID: PMC8008340.

23. Planas D, Veyer D, Baidaliuk A, Staropoli I, Guivel-Benhassine F, Rajah MM, Planchais C, Porrot F, Robillard N, Puech J, Prot M, Gallais F, Gantner P, Velay A, Le Guen J, Kassis-Chikhani N, Edriss D, Belec L, Seve A, Courtellemont L, Pere H, Hocqueloux L, Fafi-Kremer S, Prazuck T, Mouquet H, Bruel T, Simon-Loriere E, Rey FA, Schwartz O. Reduced sensitivity of SARS-CoV-2 variant Delta to antibody neutralization. Nature. 2021;596(7871):276-80. Epub 20210708. doi: 10.1038/s41586-021-03777-9. PubMed PMID: 34237773.

24. Henderson R, Edwards RJ, Mansouri K, Janowska K, Stalls V, Gobeil SMC, Kopp M, Li D, Parks R, Hsu AL, Borgnia MJ, Haynes BF, Acharya P. Controlling the SARS-CoV-2 spike glycoprotein conformation. Nat Struct Mol Biol. 2020;27(10):925-33. Epub 20200722. doi: 10.1038/s41594-020-0479-4. PubMed PMID: 32699321; PMCID: PMC8581954.

25. Zhou T, Tsybovsky Y, Gorman J, Rapp M, Cerutti G, Chuang GY, Katsamba PS, Sampson JM, Schon A, Bimela J, Boyington JC, Nazzari A, Olia AS, Shi W, Sastry M, Stephens T, Stuckey J, Teng IT, Wang P, Wang S, Zhang B, Friesner RA, Ho DD, Mascola JR, Shapiro L, Kwong PD. Cryo-EM Structures of SARS-CoV-2 Spike without and with ACE2 Reveal a pH-Dependent Switch to Mediate Endosomal Positioning of Receptor-Binding Domains. Cell Host Microbe.

2020;28(6):867-79 e5. Epub 20201117. doi: 10.1016/j.chom.2020.11.004. PubMed PMID: 33271067; PMCID: PMC7670890.

26. Calvaresi V, Wrobel AG, Toporowska J, Hammerschmid D, Doores KJ, Bradshaw RT, Parsons RB, Benton DJ, Roustan C, Reading E, Malim MH, Gamblin SJ, Politis A. Structural dynamics in the evolution of SARS-CoV-2 spike glycoprotein. Nat Commun. 2023;14(1):1421. Epub 20230314. doi: 10.1038/s41467-023-36745-0. PubMed PMID: 36918534; PMCID: PMC10013288.

27. Schaub JM, Chou CW, Kuo HC, Javanmardi K, Hsieh CL, Goldsmith J, DiVenere AM, Le KC, Wrapp D, Byrne PO, Hjorth CK, Johnson NV, Ludes-Meyers J, Nguyen AW, Wang N, Lavinder JJ, Ippolito GC, Maynard JA, McLellan JS, Finkelstein IJ. Expression and characterization of SARS-CoV-2 spike proteins. Nat Protoc. 2021;16(11):5339-56. Epub 20211005. doi: 10.1038/s41596-021-00623-0. PubMed PMID: 34611365; PMCID: PMC9665560.

28. Turner AJ. ACE2 Cell Biology, Regulation, and Physiological Functions. The Protective Arm of the Renin Angiotensin System (RAS)2015. p. 185-9.

29. Lewis AL SC, Schnaar RL, editor. Essentials of Glycobiology. 4th Edition ed. Cold Spring Harbor, NY: Cold Spring Harbor Laboratory Press;; 2022.

30. Pandey VK, Sharma R, Prajapati GK, Mohanta TK, Mishra AK. N-glycosylation, a leading role in viral infection and immunity development. Mol Biol Rep. 2022;49(8):8109-20. Epub 20220401. doi: 10.1007/s11033-022-07359-4. PubMed PMID: 35364718; PMCID: PMC8974804.

31. Vigerust DJ, Shepherd VL. Virus glycosylation: role in virulence and immune interactions. Trends Microbiol. 2007;15(5):211-8. Epub 20070329. doi: 10.1016/j.tim.2007.03.003. PubMed PMID: 17398101; PMCID: PMC7127133.

32. Xie Y, Butler M. Quantitative profiling of N-glycosylation of SARS-CoV-2 spike protein variants. Glycobiology. 2023;33(3):188-202. doi: 10.1093/glycob/cwad007. PubMed PMID: 36723867; PMCID: PMC10114651.

33. Casalino L, Gaieb Z, Goldsmith JA, Hjorth CK, Dommer AC, Harbison AM, Fogarty CA, Barros EP, Taylor BC, McLellan JS, Fadda E, Amaro RE. Beyond Shielding: The Roles of Glycans in the SARS-CoV-2 Spike Protein. ACS Cent Sci. 2020;6(10):1722-34. Epub 20200923. doi: 10.1021/acscentsci.0c01056. PubMed PMID: 33140034; PMCID: PMC7523240.

34. Zhao P, Praissman JL, Grant OC, Cai Y, Xiao T, Rosenbalm KE, Aoki K, Kellman BP, Bridger R, Barouch DH, Brindley MA, Lewis NE, Tiemeyer M, Chen B, Woods RJ, Wells L. Virus-Receptor Interactions of Glycosylated SARS-CoV-2 Spike and Human ACE2 Receptor. Cell Host Microbe. 2020;28(4):586-601 e6. Epub 20200824. doi: 10.1016/j.chom.2020.08.004. PubMed PMID: 32841605; PMCID: PMC7443692.

35. Gstottner C, Zhang T, Resemann A, Ruben S, Pengelley S, Suckau D, Welsink T, Wuhrer M, Dominguez-Vega E. Structural and Functional Characterization of SARS-CoV-2 RBD Domains Produced in Mammalian Cells. Anal Chem. 2021;93(17):6839-47. Epub 20210419. doi: 10.1021/acs.analchem.1c00893. PubMed PMID: 33871970; PMCID: PMC8078197.

36. Mittal A, Khattri A, Verma V. Structural and antigenic variations in the spike protein of emerging SARS-CoV-2 variants. PLoS Pathog. 2022;18(2):e1010260. Epub 20220217. doi: 10.1371/journal.ppat.1010260. PubMed PMID: 35176090; PMCID: PMC8853550.

37. Zhu R, Canena D, Sikora M, Klausberger M, Seferovic H, Mehdipour AR, Hain L, Laurent E, Monteil V, Wirnsberger G, Wieneke R, Tampe R, Kienzl NF, Mach L, Mirazimi A, Oh YJ, Penninger JM, Hummer G, Hinterdorfer P. Force-tuned avidity of spike variant-ACE2 interactions viewed on the single-molecule level. Nat Commun. 2022;13(1):7926. Epub 20221224. doi: 10.1038/s41467-022-35641-3. PubMed PMID: 36566234; PMCID: PMC9789309.

38. Zhang F, Schmidt F, Muecksch F, Wang Z, Gazumyan A, Nussenzweig MC, Gaebler C, Caskey M, Hatziioannou T, Bieniasz PD. SARS-CoV-2 spike glycosylation affects function and neutralization sensitivity. mBio. 2024;15(2):e01672-23. doi: doi:10.1128/mbio.01672-23.

39. Isobe A, Arai Y, Kuroda D, Okumura N, Ono T, Ushiba S, Nakakita SI, Daidoji T, Suzuki Y, Nakaya T, Matsumoto K, Watanabe Y. ACE2 N-glycosylation modulates interactions with SARS-CoV-2 spike protein in a site-specific manner. Commun Biol. 2022;5(1):1188. Epub 20221105. doi: 10.1038/s42003-022-04170-6. PubMed PMID: 36335195; PMCID: PMC9637154.

40. Lamers MM, Haagmans BL. SARS-CoV-2 pathogenesis. Nat Rev Microbiol. 2022;20(5):270-84. Epub 20220330. doi: 10.1038/s41579-022-00713-0. PubMed PMID: 35354968.

41. Jones JE, Le Sage V, Lakdawala SS. Viral and host heterogeneity and their effects on the viral life cycle. Nat Rev Microbiol. 2021;19(4):272-82. Epub 20201006. doi: 10.1038/s41579-020-00449-9. PubMed PMID: 33024309; PMCID: PMC7537587.

42. Minkoff JM, tenOever B. Innate immune evasion strategies of SARS-CoV-2. Nat Rev Microbiol. 2023;21(3):178-94. Epub 20230111. doi: 10.1038/s41579-022-00839-1. PubMed PMID: 36631691; PMCID: PMC9838430.

43. El-Baba TJ, Lutomski CA, Burnap SA, Bolla JR, Baker LA, Baldwin AJ, Struwe WB, Robinson CV. Uncovering the Role of N-Glycan Occupancy on the Cooperative Assembly of Spike and Angiotensin Converting Enzyme 2 Complexes: Insights from Glycoengineering and Native Mass Spectrometry. J Am Chem Soc. 2023;145(14):8021-32. Epub 20230331. doi: 10.1021/jacs.3c00291. PubMed PMID: 37000485; PMCID: PMC10103161.

44. Rowland R, Brandariz-Nunez A. Analysis of the Role of N-Linked Glycosylation in Cell Surface Expression, Function, and Binding Properties of SARS-CoV-2 Receptor ACE2. Microbiol Spectr. 2021;9(2):e0119921. Epub 20210908. doi: 10.1128/Spectrum.01199-21. PubMed PMID: 34494876; PMCID: PMC8557876.

45. Focosi D, Maggi F. Neutralising antibody escape of SARS-CoV-2 spike protein: Risk assessment for antibody-based Covid-19 therapeutics and vaccines. Rev Med Virol. 2021;31(6):e2231. Epub 20210316. doi: 10.1002/rmv.2231. PubMed PMID: 33724631; PMCID: PMC8250244.

46. Cueno ME, Imai K. Structural Comparison of the SARS CoV 2 Spike Protein Relative to Other Human-Infecting Coronaviruses. Front Med (Lausanne). 2020;7:594439. Epub 20210114. doi: 10.3389/fmed.2020.594439. PubMed PMID: 33585502; PMCID: PMC7874069.

47. Grant OC, Montgomery D, Ito K, Woods RJ. Analysis of the SARS-CoV-2 spike protein glycan shield reveals implications for immune recognition. Sci Rep. 2020;10(1):14991. Epub 20200914. doi: 10.1038/s41598-020-71748-7. PubMed PMID: 32929138; PMCID: PMC7490396.

48. Haycroft ER, Davis SK, Ramanathan P, Lopez E, Purcell RA, Tan LL, Pymm P, Wines BD, Hogarth PM, Wheatley AK, Juno JA, Redmond SJ, Gherardin NA, Godfrey DI, Tham WH,

Selva KJ, Kent SJ, Chung AW. Antibody Fc-binding profiles and ACE2 affinity to SARS-CoV-2 RBD variants. Med Microbiol Immunol. 2023;212(4):291-305. Epub 20230721. doi: 10.1007/s00430-023-00773-w. PubMed PMID: 37477828; PMCID: PMC10372118.

49. Yi C, Sun X, Ye J, Ding L, Liu M, Yang Z, Lu X, Zhang Y, Ma L, Gu W, Qu A, Xu J, Shi Z, Ling Z, Sun B. Key residues of the receptor binding motif in the spike protein of SARS-CoV-2 that interact with ACE2 and neutralizing antibodies. Cell Mol Immunol. 2020;17(6):621-30. Epub 20200515. doi: 10.1038/s41423-020-0458-z. PubMed PMID: 32415260; PMCID: PMC7227451.

50. Andreano E, Piccini G, Licastro D, Casalino L, Johnson NV, Paciello I, Dal Monego S, Pantano E, Manganaro N, Manenti A, Manna R, Casa E, Hyseni I, Benincasa L, Montomoli E, Amaro RE, McLellan JS, Rappuoli R. SARS-CoV-2 escape from a highly neutralizing COVID-19 convalescent plasma. Proc Natl Acad Sci U S A. 2021;118(36). doi: 10.1073/pnas.2103154118. PubMed PMID: 34417349; PMCID: PMC8433494.

51. Cao Y, Su B, Guo X, Sun W, Deng Y, Bao L, Zhu Q, Zhang X, Zheng Y, Geng C, Chai X, He R, Li X, Lv Q, Zhu H, Deng W, Xu Y, Wang Y, Qiao L, Tan Y, Song L, Wang G, Du X, Gao N, Liu J, Xiao J, Su XD, Du Z, Feng Y, Qin C, Qin C, Jin R, Xie XS. Potent Neutralizing Antibodies against SARS-CoV-2 Identified by High-Throughput Single-Cell Sequencing of Convalescent Patients' B Cells. Cell. 2020;182(1):73-84 e16. Epub 20200518. doi: 10.1016/j.cell.2020.05.025. PubMed PMID: 32425270; PMCID: PMC7231725.

52. Wu WL, Chiang CY, Lai SC, Yu CY, Huang YL, Liao HC, Liao CL, Chen HW, Liu SJ. Monoclonal antibody targeting the conserved region of the SARS-CoV-2 spike protein to overcome viral variants. JCI Insight. 2022;7(8). Epub 20220422. doi: 10.1172/jci.insight.157597. PubMed PMID: 35290246; PMCID: PMC9089791.

53. Focosi D, McConnell S, Casadevall A, Cappello E, Valdiserra G, Tuccori M. Monoclonal antibody therapies against SARS-CoV-2. Lancet Infect Dis. 2022;22(11):e311-e26. Epub 20220705. doi: 10.1016/S1473-3099(22)00311-5. PubMed PMID: 35803289; PMCID: PMC9255948.

54. Peter AS, Gruner E, Socher E, Fraedrich K, Richel E, Mueller-Schmucker S, Cordsmeier A, Ensser A, Sticht H, Uberla K. Characterization of SARS-CoV-2 Escape Mutants to a Pair of Neutralizing Antibodies Targeting the RBD and the NTD. Int J Mol Sci. 2022;23(15). Epub 20220725. doi: 10.3390/ijms23158177. PubMed PMID: 35897753; PMCID: PMC9332373.

55. Starr TN, Greaney AJ, Dingens AS, Bloom JD. Complete map of SARS-CoV-2 RBD mutations that escape the monoclonal antibody LY-CoV555 and its cocktail with LY-CoV016. Cell Rep Med. 2021;2(4):100255. Epub 20210405. doi: 10.1016/j.xcrm.2021.100255. PubMed PMID: 33842902; PMCID: PMC8020059.

56. Weisblum Y, Schmidt F, Zhang F, DaSilva J, Poston D, Lorenzi JC, Muecksch F, Rutkowska M, Hoffmann HH, Michailidis E, Gaebler C, Agudelo M, Cho A, Wang Z, Gazumyan A, Cipolla M, Luchsinger L, Hillyer CD, Caskey M, Robbiani DF, Rice CM, Nussenzweig MC, Hatziioannou T, Bieniasz PD. Escape from neutralizing antibodies by SARS-CoV-2 spike protein variants. Elife. 2020;9. Epub 20201028. doi: 10.7554/eLife.61312. PubMed PMID: 33112236; PMCID: PMC7723407.

57. Newby ML, Fogarty CA, Allen JD, Butler J, Fadda E, Crispin M. Variations within the Glycan Shield of SARS-CoV-2 Impact Viral Spike Dynamics. J Mol Biol. 2023;435(4):167928. Epub 20221221. doi: 10.1016/j.jmb.2022.167928. PubMed PMID: 36565991; PMCID: PMC9769069.

58. Hsiao YW, Bray DJ, Taddese T, Jimenez-Serratos G, Crain J. Structure adaptation in Omicron SARS-CoV-2/hACE2: Biophysical origins of evolutionary driving forces. Biophys J. 2023;122(20):4057-67. Epub 20230916. doi: 10.1016/j.bpj.2023.09.003. PubMed PMID: 37717145; PMCID: PMC10624932.

59. Singh A, Steinkellner G, Kochl K, Gruber K, Gruber CC. Serine 477 plays a crucial role in the interaction of the SARS-CoV-2 spike protein with the human receptor ACE2. Sci Rep. 2021;11(1):4320. Epub 20210222. doi: 10.1038/s41598-021-83761-5. PubMed PMID: 33619331; PMCID: PMC7900180.

60. Wrobel AG, Benton DJ, Hussain S, Harvey R, Martin SR, Roustan C, Rosenthal PB, Skehel JJ, Gamblin SJ. Antibody-mediated disruption of the SARS-CoV-2 spike glycoprotein. Nat Commun. 2020;11(1):5337. Epub 20201021. doi: 10.1038/s41467-020-19146-5. PubMed PMID: 33087721; PMCID: PMC7577971.

61. Pettersen EF, Goddard TD, Huang CC, Meng EC, Couch GS, Croll TI, Morris JH, Ferrin TE. UCSF ChimeraX: Structure visualization for researchers, educators, and developers. Protein Sci. 2021;30(1):70-82. Epub 20201022. doi: 10.1002/pro.3943. PubMed PMID: 32881101; PMCID: PMC7737788.